

RESEARCH ARTICLE

Open Access



# Cool, alkaline serpentinite formation fluid regime with scarce microbial habitability and possible abiotic synthesis beneath the South Chamorro Seamount

Shinsuke Kawagucci<sup>1,5\*</sup> , Junichi Miyazaki<sup>1</sup>, Yuki Morono<sup>2</sup>, Jeff S. Seewald<sup>3</sup>, C. Geoff Wheat<sup>4</sup> and Ken Takai<sup>1</sup>

## Abstract

South Chamorro Seamount (SCS) is a blueschist-bearing serpentinite mud volcano in the Mariana forearc. Previous scientific drilling conducted at SCS revealed highly alkaline, sulfate-rich formation fluids resulting from slab-derived fluid upwelling combined with serpentinization both beneath and within the seamount. In the present study, a time-series of ROV dives spanning 1000 days was conducted to collect discharging alkaline fluids from the cased Ocean Drilling Program (ODP) Hole 1200C (hereafter the CORK fluid). The CORK fluids were analyzed for chemical compositions (including dissolved gas) and microbial community composition/function. Compared to the ODP porewater, the CORK fluids were generally identical in concentration of major ions, with the exception of significant sulfate depletion and enrichment in sulfide, alkalinity, and methane. Microbiological analyses of the CORK fluids revealed little biomass and functional activity, despite habitable temperature conditions. The post-drilling sulfate depletion is likely attributable to sulfate reduction coupled with oxidation of methane (and hydrogen), probably triggered by the drilling and casing operations. Multiple lines of evidence suggest that abiotic organic synthesis associated with serpentinization is the most plausible source of the abundant methane in the CORK fluid. The SCS formation fluid regime presented here may represent the first example on Earth where abiotic syntheses are conspicuous with little biotic processes, despite a condition with sufficient bioavailable energy potentials and temperatures within the habitable range.

**Keywords:** Forearc serpentinite mud volcano, South Chamorro Seamount, Limit of biosphere, Present-days' chemical evolution, Radio-isotope-tracer carbon assimilation estimation

## Introduction

Serpentinization of ultramafic rocks that are the major components of the oceanic lithosphere produces highly reductive fluids, in which transformation of inorganic carbon species to organic matter occur (e.g., McCollom 2013). Serpentinization-associated geofluid systems have been recognized as modern analogs of plausible settings for the origin of primordial life (e.g., Russell et al. 2014) as well as ancient microbial communities (e.g., Takai et al. 2006; Ueda

et al. 2016). Serpentinization-associated geofluid systems, typically characterized by an abundance of H<sub>2</sub> and/or highly alkaline fluids, have been discovered at a range of tectonic/geological settings on the modern Earth where ultramafic rocks encounter water circulation. The most notable examples include slow-spreading mid-oceanic ridges (Charlou et al. 2002; Konn et al. 2015), ocean core complexes (Kelley et al. 2001; Früh-Green et al. 2003), ophiolites (Barnes et al. 1978; Schrenk et al. 2013), coastal springs (Barnes et al. 1967), onshore volcanic hot springs (Homma and Tsukahara, 2008; Suda et al. 2014), inner trench slope along the southern Mariana forearc (Ohara et al. 2012; Okumura et al. 2016a; Onishi et al. 2018), and forearc serpentinite seamounts (Mottl et al. 2004; Fryer, 2011).

\* Correspondence: [kawagucci@jamstec.go.jp](mailto:kawagucci@jamstec.go.jp)

<sup>1</sup>Department of Subsurface Geobiological Analysis and Research (D-SUGAR), Japan Agency for Marine-Earth Science and Technology (JAMSTEC), 2-15 Natsushima-cho, Yokosuka 237-0061, Japan

<sup>5</sup>Institute of Geochemistry and Petrology, ETH Zürich, Zürich, Switzerland

Full list of author information is available at the end of the article

Forearc serpentinite mud volcanoes are formed by extensive serpentinization of the mantle, triggered by the injection of slab-derived fluids into the overlying mantle wedge in a subduction setting. These serpentinization products ascend to form the largest mud volcanoes on Earth (Fryer, 2011). Deep-sea serpentinite mud volcanoes are outstanding settings, compared to other serpentinization-associated geofluid systems (Table 1), for studying abiotic organic syntheses (i.e., present-days' chemical evolution) and for finding the boundary between microbiologically habitable and uninhabitable zones (i.e., limit of life and the biosphere) in natural environments of the Earth. For example, the impermeable mud volcano allows for decreased entrainment of photosynthesis-derived organic matter and seawater-derived microbial populations into the internal part of the volcano where pristine mud and fluid ascend from the deep. As such, if we can obtain these pristine fluids contributing to the formation of serpentinite mud volcanoes, then they can be used to address the unique geochemical and microbiological processes associated with these volcanoes.

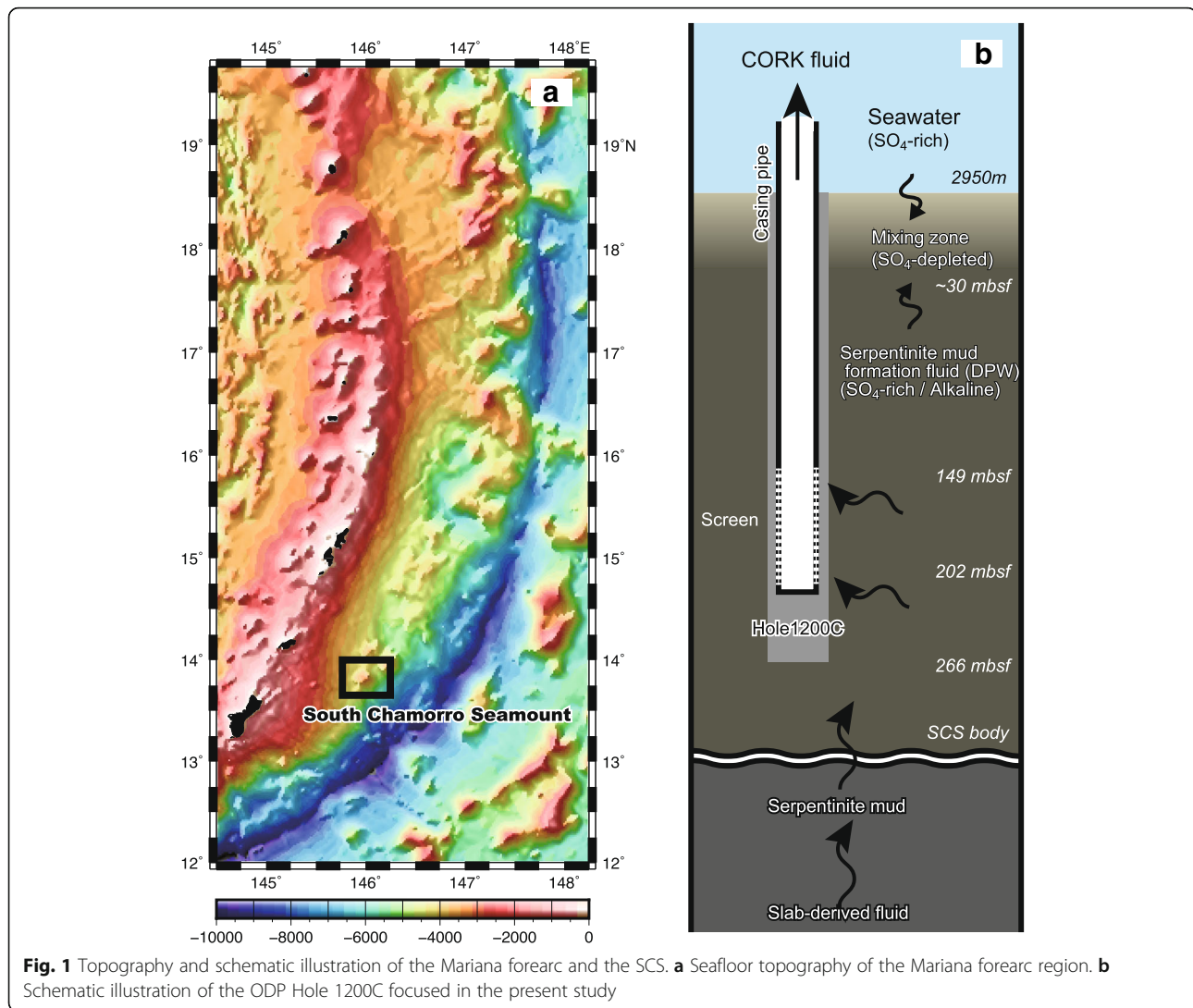
The South Chamorro Seamount (SCS) is located at the southern end of a serpentinite mud volcano chain in the Mariana forearc, where the Pacific plate subducts beneath the Philippine Sea plate (Fig. 1a). To date, the SCS is the only known location of active blueschist-bearing serpentinite mud volcanism that hosts lush deep-sea chemosynthetic communities sustained by the serpentinite fluid seepage (Fryer and Mottl, 1997). The Ocean Drilling Program (ODP) Leg 195 drilled the summit of the SCS (Site 1200) in 2001 and obtained core samples in order to examine

geological and biogeochemical processes associated with subduction (Shipboard Sci. Party 2002). The serpentinite mud porewater, with the exception of taken near the seafloor, exhibited a highly basic pH of 12.5 and had a composition rich in dissolved sulfate and carbonate. The alkaline porewater chemistry is indicative of slab-derived fluids that had reacted with mantle rocks when ascending through the overlying plate (Fig. 1b), but few studies have investigated the origin of the abundant sulfate in the deep (Mottl et al. 2003, 2004; Hulme et al. 2010). In addition, porewater samples from shallow zones ~ 20 mbsf exhibited sulfate depletion and high alkalinity. The chemistry of these shallow fluids has been interpreted to reflect the oxidation of CH<sub>4</sub> (and H<sub>2</sub>) derived from the deep by a shallow, sub-seafloor microbial community including sulfate-reducers (Mottl et al. 2003; Aoyama et al. 2018). However, the gas composition of the porewater could not be accurately determined, since the standard ODP sampling retrieval, handling, and on-board procedures resulted in a significant loss of dissolved gases. Microbiological analyses including phospholipid analysis (Mottl et al. 2003), cell count, and cultivation attempts (Takai et al. 2005) were carried out, but the community structure and potential microbial functions could not be determined.

A cased borehole observatory, the Circulation Obviation Retrofit Kit (CORK), was deployed during the ODP Leg 195 at Hole 1200C on the SCS (Shipboard Sci. Party 2002; Wheat et al. 2008). When the observatory seal was opened on 20 March 2003, 2 years after its installation, over-pressurized fluids discharged from the CORK outlet

**Table 1** Deep-sea serpentinization-associated geofluid fields

Name of field	South Chamorro Seamount (SCS)	Shinkai Seep Field	Lost City	Rainbow
Location	13°47'N–146°00'E	11°40'N–140°03'E	30°07'N–42°07'W	36°14'N–33°54'W
Tectonics	Forearc seamount chain	Non-accretionary trench slope	Oceanic core complex, MAR	Non-transform offset, MAR
Driving force	Serpentine mud volcanism	(Hydrothermalism?)	Hydrothermalism	Hydrothermalism
Fluid source	Slab-derived fluid	Seawater penetration	Seawater penetration	Seawater penetration
Approach	ODP, CORK, Dive	Dive	Dive, IODP	Dive
Depth (m)	2960	5800	700–800	2300
T max	2	–	> 91	365
pH	12.5	(Brucite chimney)	10.7	2.8
H <sub>2</sub> (mM)	0.01 (possibly < 40)	–	15	16
CH <sub>4</sub> (mM)	37 (possibly < 65)	–	2	2.5
Note	The strongest alkaline deep-sea geofluid system so far identified. See text for details.	Active alkaline fluid seeping from brucite chimney surrounded by macrofauna colony.	Hot alkaline fluid discharging from tall carbonate chimney, only identified on the modern seafloor at this moment.	Black smoker acidic fluid discharging from sulfide chimney with abundant H <sub>2</sub> . Similar vent sites have already been found on the modern seafloor.
Ref	See text	Ohara et al. 2012 Stern et al. 2014 Okumura et al., 2016a Onishi et al. 2018	Kelley et al. 2001 Früh-Green et al. 2003 Proskurowski et al. 2008	Charlou et al. 2002



pipe (this fluid is referred to as the ‘CORK fluid’ hereafter) at a flow rate of  $\sim 0.2$  L/s. The endmember chemical composition of the CORK fluid, estimated from two fluid samples diluted with entrained ambient seawater, was generally similar to those from the porewater samples from deeper zones of the ODP core (Wheat et al. 2008). Although the deep porewater samples obtained during the ODP Leg 195 in 2001 contained abundant sulfate and negligible sulfide, sulfide was present in the highly alkaline (pH 12.4) CORK fluid. This difference implies that partial reduction of sulfate to sulfide could occur within the SCS mud volcano before the formation fluid discharged through the cased borehole (Wheat et al. 2008). Discharge from the open borehole continued for 37 days, until the observatory was resealed on 28 April 2003. During the 2003 campaign, however, no gas-tight fluid sampling was conducted despite gas species such as  $H_2$ ,  $CO$ ,  $CH_4$ , and other hydrocarbons are key chemical clues for investigating both abiotic organic synthesis and microbiological habitability/function in an active serpentinite mud volcano.

The present study presents results from four subsequent sample collection campaigns utilizing remotely operated vehicle (ROV) dives with gas-tight fluid samplers (Seewald et al. 2001; Saegusa et al. 2006) and other sampling tools conducted between 2009 and 2012 to collect fresh fluids discharging from the cased borehole of Hole 1200C. The chemistry of the CORK fluid, particularly dissolved gas species, as well as the microbial community composition and function were determined. Carbon and sulfur compositions in the CORK fluids were altered from those from the ODP porewater samples, probably due to changes in the subseafloor hydrological field before and after the scientific drilling event. Analyses of the CORK fluids and the ODP porewater suggested that the sulfate-methane couple likely co-exist in the native SCS formation fluid. However, low biomass and activity were observed environments where physical and chemical conditions, particularly the temperature ( $\sim 3$  °C) and bioavailable energy

potentials, were suitable for supporting a prosperous microbial community. Multiple lines of evidence, such as low microbial biomass and activity, point to abiotic hydrocarbon synthesis associated with serpentinization occurring beneath the SCS.

## Methods/experimental

### Site description

In 2001, a series of boreholes were drilled near the seepage sites at the summit of the SCS (ODP Site 1200) (Shipboard Sci. Party 2002). The ODP Hole 1200C was drilled to 266 mbsf prior to casing and the installation of a CORK device. The final configuration was placed at the base of the casing at 202.8 mbsf, providing a screened section from 148.8 mbsf to 202.3 mbsf (Fig. 1b). On 20 March 2003, the CORK monitoring instruments were recovered using the ROV Jason II, and on 28 April 2003 the top of the CORK was resealed by a steel housing holding a downhole pressure sensor (Wheat et al. 2008).

### Sampling and analysis

#### Fluid sampling

CORK fluids were collected for both chemical characterization and analyses of microbial biomass/function during four cruises of the R/V Natsushima with ROV Hyper-Dolphin in January 2009 (NT09-01, HPD#941-947), May–June 2009 (NT09-07, HPD#1007-1010), February 2012 (NT12-04, HPD#1349-1350), and September 2012 (NT12-23, HPD#1433-1434). On 20 January 2009 (HPD#941), the valve on the original-type CORK was opened. The discharging fluid (#941) appeared blackish in coloration, probably due to suspension of sulfide minerals that had accumulated during the past 6 years. The likely source for this blackish fluid is the discharging fluid that occupied the pipe casing when the valve was closed in 2003. After initial samples were collected, the steel plug was replaced with a polyvinyl chloride (PVC) tube and a ball valve. This PVC tube was inserted past the latch holes in the CORK body, sealing the borehole from the bottom seawater. Thus, fluids collected from the top of the CORK can be considered pristine CORK fluids with minimal or no entrainment of the bottom seawater (Wheat et al. 2008). Fluid collected during subsequent dives appeared to be colorless and clear at the mouth of the CORK but the coloration changed to whitish after venting, most likely due to the precipitation of brucite from seawater-derived  $Mg^{2+}$  and CORK fluid-derived  $OH^-$ .

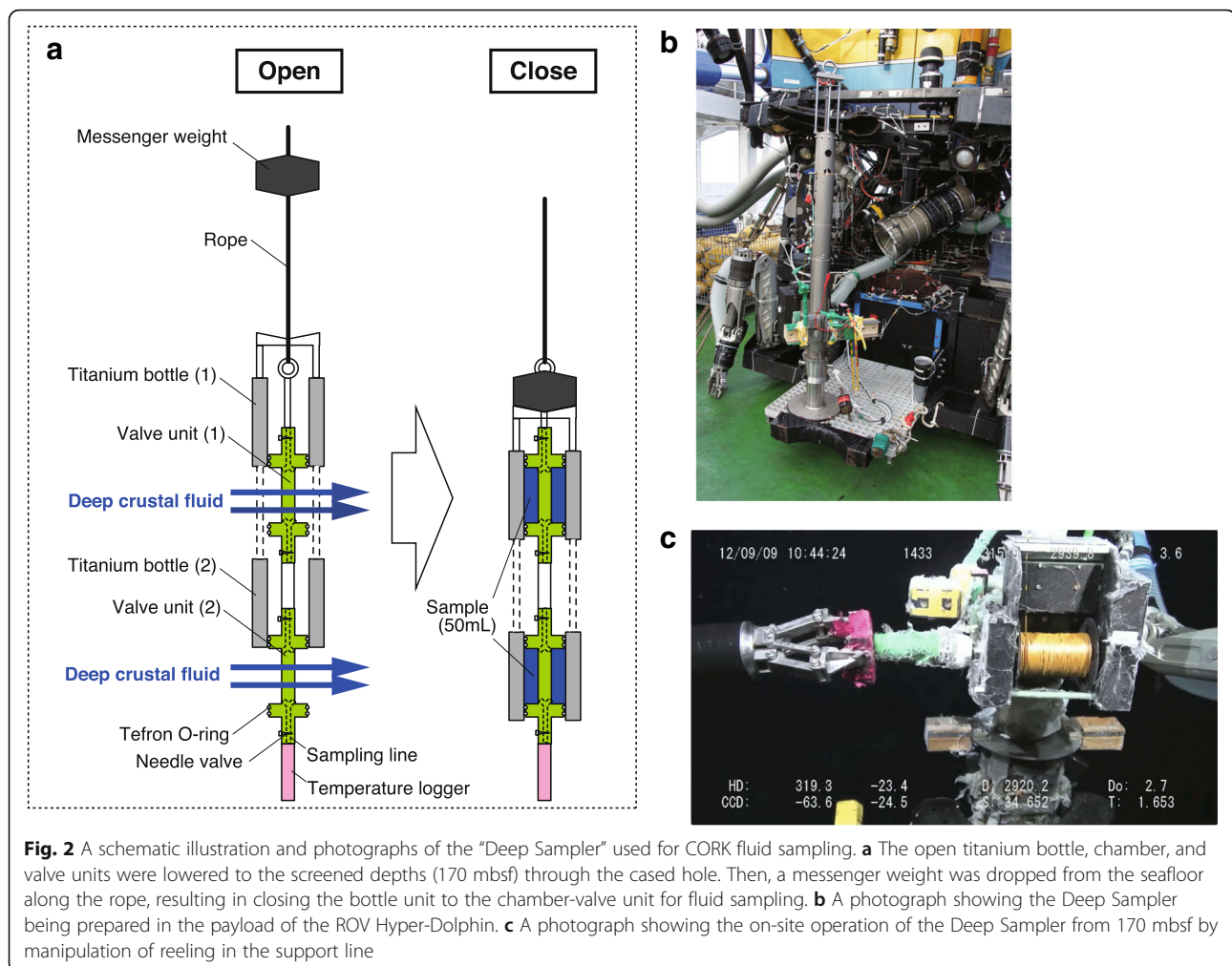
CORK fluids were collected using several types of fluid samplers, including WHATS, Bag, and Isobaric Gas-Tight (IGT) samplers (Seewald et al. 2001; Saegusa et al. 2006). The whitish fluids were also collected into pre-evacuated stainless-steel bottles with radio-isotope-labeled tracers for metabolic activity measurements (see below). The inlet

nozzles for WHATS and Bag samplers were inserted as deep as possible into the borehole in order to minimize seawater contamination. For fluids collected using IGT samplers, a polycarbonate reservoir was attached to the CORK ball valve. The reservoir was flushed with several volumes of CORK fluid before the IGT sampler snorkel was inserted into the reservoir through a rubber diaphragm to collect pristine CORK fluid without seawater entrainment.

A special sampling device, named the “Deep Sampler,” was also used during cruises NT12-04 and NT12-23 to collect fluid within the borehole at subsurface depths where the screened casing is positioned (Fig. 2). The Deep Sampler consisted of a 100 mL gas-tight and pressure-preserved titanium bottle and a valve connected to a winch on the seafloor with a rope. The open titanium bottle-chamber-valve units were lowered to a depth of 179 mbsf within the depth range of the screens, before a messenger weight was dropped from the seafloor to slide the bottle unit to the chamber-valve unit for fluid sampling (a few seconds to 10 s time) and in the end sealing the fluid in two of the chambers (Fig. 2). The temperature was monitored during fluid sampling, which increased from  $\sim 1.7$  °C at the seafloor to 3.3 °C at 170 m below the seafloor (thermal gradient of 9.4 °C/km). Samples collected by the Deep Sampler and the other samplers did not show significant differences in their chemical composition, implying that fluid alteration and seawater contamination during the 12 h ascent through the cased hole (Wheat et al. 2008) was negligible.

#### Geochemistry

Immediately upon recovery of the ROV, fluid samples were subsampled for liquid and gas analyses. For liquid phase analysis, the fluid sample was withdrawn into disposable plastic syringes for filtration, and then introduced into acid-washed HDPE bottles and glass vials. Shipboard measurements included pH, alkalinity, chlorinity, and hydrogen sulfide. Shore-based analyses with devices such as ion chromatography (IC), inductively coupled plasma atomic emission spectrometry (ICP-AES), and ICP mass spectrometry (ICP-MS) were conducted using techniques similar to those carried out for the ODP 1200 porewater samples (e.g., Mottl et al. 2003, 2004), thus minimizing analytical biases among these studies. Dissolved gas extraction from fluid samples collected with the WHATS sampler was conducted using previously reported techniques (e.g., Kawagucci et al. 2016; Miyazaki et al. 2017). To extract the total inorganic carbon (mainly  $CO_3^{2-}$ ) as  $CO_2$  for abundance and isotope analyses, the fluid sample was acidified with  $\sim 3$  g of solid sulfamic acid ( $H_3NSO_3$ ) in the extraction line. While the total gas content was determined barometrically during the gas extraction, the relative abundance of  $H_2$ ,  $CH_4$ ,  $CO$ ,  $CO_2$ ,  $C_2H_6$ , and  $C_3H_8$  in the whole gas phase were determined by gas chromatography using a helium ionization detector. The



stable isotopic compositions of  $H_2$ ,  $CH_4$ ,  $CO_2$ , and  $C_2H_6$  were determined using the continuous flow method with DELTA XP Advantage and/or MAT253 Isotope Ratio Mass Spectrometer (Thermo Fisher Scientific) in JAMSTEC in accordance with previously published techniques (e.g., Okumura et al. 2016b; Shibuya et al. 2017). In the present study, isotope ratio and isotope fractionation between two molecules is represented by conventional  $\delta$  and  $\alpha$  notations as  $\delta^{13}C_A = [(^{13}C_A/^{12}C_A)/(^{13}C_{STD}/^{12}C_{STD}) - 1]$  (presented in permil scale) and  $\alpha_{C_A-B} = (\delta^{13}C_A + 1)/(\delta^{13}C_B + 1)$ . Samples collected using IGT samplers were analyzed at sea for dissolved  $H_2$  and  $CH_4$  using gas chromatography with thermal conductivity detection, following headspace extraction.

### Microbiology

During cruises NT09-01 and NT09-07, microbial cells in subsampled fluids (110–370 mL) were collected on-board the ship onto 0.2  $\mu m$  pore 47 mm polycarbonate membranes (K020A047A, ADVANTEC, Tokyo Japan) placed in line holder (KS-47, ADVANTEC, Tokyo Japan). The cells were fixed by placing a fixation solution

(2% paraformaldehyde-PBS solution) onto the membranes and kept overnight at 4 °C. Then, the membrane was washed by PBS, partially dried by placing on filter paper, and kept at –20 °C for later cell counting. The fluid sample taken on the cruise NT12-23 was immediately fixed by adding 1/5 volume of 10% Formalin Neutral Buffer Solution (Wako, Japan) and stored at 4 °C until further processing. Since white precipitates formed in fixed fluid samplers during storage at 4 °C, separation of cells was conducted according to Morono et al. (2013), with some modifications. In brief, for 3–15 mL of fixed solution, 1/10 volume each of detergent mix (100 mM EDTA, 100 mM sodium pyrophosphate, 1% [v/v] Tween 80) and methanol were added and treated in an ultrasonic bath (Bioruptor UCD-250, Cosmo Bio, Tokyo Japan) at 160 W with cycles of 1 min ON and 1 min OFF for 20 min. The treated samples were then carefully layered onto step gradient heavy density solution composed of 67% (w/w) sodium polytungstate (SPT1, SOMETU, Berlin, Germany), 80%, 50%, and 30% (w/v) Nycodenz and centrifuged for 120 min at 10,000 $\times g$

at 25 °C. Light density upper layers were recovered, and 10% of the suspension was passed through a 0.2 µm pore 25 mm polycarbonate membrane to trap microbial cells. The filters were stored at -20 °C until counting. From Bag sampler (NT09-01) and Deep Sampler (NT12-23), about 10 L and 40 mL of fluids, respectively, were filtered with 0.22 µm-pore-sized cellulose acetate filters to collect microbial cells. Filters were stored at -80 °C for microbial 16S rRNA gene clone sequencing analysis.

Microbial cell densities in CORK fluid samples were determined using a semi-automated cell counting system (Morono et al. 2009). In brief, trapped and fixed cells collected on a polycarbonate membrane were stained with SYBR green I staining solution (1/40 [v/v] SYBR Green I in TE buffer). The stained filter was washed with 1 ml of TE buffer and then mounted on a glass microscope slide with 3–5 µL of mounting solution (2:1 mixture of VECTASHIELD mounting medium H-1000 and TE buffer). Microscopic fluorescence image acquisition (at 525/36 nm [center wavelength/bandwidth] and 605/52 nm by 490 nm excitation) was performed automatically using a fluorescence microscope equipped with an automatic slide handler (Morono and Inagaki, 2010). The resulting images were analyzed using the macro of the Metamorph software (Molecular Devices, CA, USA) to identify and count microbial cells on the membrane.

Phylotype composition of 16S rRNA genes were determined using clone sequencing in the laboratory based on a previously published methodology (Nunoura et al. 2012) with some modifications. DNA assemblages were extracted from microbial cells on filters using the UltraClean Soil DNA Isolation Kit (MO BIO Laboratories, Carlsbad, CA, USA). Amplification of 16S rRNA genes from the extracted DNA assemblage was accomplished by a Polymerase Chain Reaction (PCR) method with LA Taq polymerase (Takara Bio, Otsu, Japan) using a primer set of 530F/907R. The amplified 16S rRNA gene fragments were applied to electrophoresis and cleaned up with a QIA quick Gel extraction Kit (QIAGEN, Valencia, CA, USA). The 16S rRNA gene clone libraries were constructed using the TA cloning kit (Invitrogen, Carlsbad, CA, USA). The nucleotide sequences of randomly selected clones were determined with a BigDye Terminator version 3.1 sequencing kit (Applied Biosystems, Foster City, CA, USA) using M13M4 (5'-GTTTTCCAGTCACGAC-3') and M13RV (5'-TGTGGAATTGTGAGCGG-3') primers on an ABI PRISM 3730xl Genetic analyzer (Applied Biosystems, Foster City, CA, USA). The sequences were assembled with Sequencher Ver. 4.8 software (Gene Code Corporation, Ann Arbor, MI, USA). The most similar reference sequences were retrieved from RDP and the GenBank database. The nucleotide sequences obtained were deposited to DDBJ (DNA data bank of Japan) with accession numbers LC279286-LC279362.

### Radio isotope tracer experiment to estimate potential metabolic rates

Potential activities of microbial assimilations of bicarbonate, methane, carbon monoxide, formate, acetate, and leucine (autotrophic, methanotrophic, carboxydo-trophic, and heterotrophic activities, respectively) were estimated by radio isotope tracer experiment using CORK fluid samples obtained during the expeditions NT09-01 and NT09-07. The CORK fluid was collected in multiple evacuated 150 mL stainless-steel bottles, each connected to a three-way valve and a sampling nozzle. All surfaces of the bottle, valve, and nozzle were treated with SilcoNert coating (Silcotek Corporation, Bellefonte, PA, USA) to avoid direct contact between the fluid and stainless steel. The sampling was conducted in duplicates for each of the radio isotope tracers. Prior to the seafloor sampling by the ROV, each of the radio-isotope-tracers ( $\text{NaH}^{14}\text{CO}_3$ ,  $^{14}\text{CH}_4$ ,  $^{14}\text{CO}$ ,  $\text{H}^{14}\text{COONa}$ ,  $^{14}\text{CH}_3^{14}\text{COONa}$ ,  $^{14}\text{C}$ -leucine) was placed in two bottles (with and without formaldehyde at a final concentration of 4%) as solution ( $\text{NaH}^{14}\text{CO}_3$ ,  $\text{H}^{14}\text{COONa}$ ,  $^{14}\text{CH}_3^{14}\text{COONa}$ ,  $^{14}\text{C}$ -leucine and formaldehyde) or gas ( $^{14}\text{CH}_4$  and  $^{14}\text{CO}$ ) in sealed glass ampoules. The final radioactivity level was 0.25 MBq per bottle. In order to assess the methanotrophic activity, three treatments were used: (i) only  $^{14}\text{CH}_4$  added, (ii)  $^{14}\text{CH}_4$  and  $\text{O}_2$  (a final concentration of 40 µM  $\text{O}_2$ ) added, and (iii)  $^{14}\text{CH}_4$  and  $\text{Na}_2\text{SO}_4$  and  $\text{Na}_2\text{S}$  (final concentrations of 10 mM and 0.5 mM, respectively) added. The additional  $\text{O}_2$  or  $\text{Na}_2\text{SO}_4$  and  $\text{Na}_2\text{S}$  were introduced either as a gas or as a solution sealed in a glass ampoule. The final concentrations of  $^{14}\text{C}$ -labeled tracers in the bottles were estimated to be about 0.1 mM, 0.4 mM, 0.4 mM, 0.1 mM, 0.1 mM, and 0.1 mM for bicarbonate, methane, carbon monoxide, formate, acetate, and leucine, respectively. After placing the radio isotope tracer into the bottle with three stainless-steel balls, the bottle was evacuated with a vacuum pump. The bottle was then sealed and shaken, which resulted in the stainless-steel balls rapturing the glass ampoules containing the radio-isotope-tracers and formaldehyde. At the seafloor, the sampling nozzle of the radio-isotope-tracer sampler was placed in the discharging CORK fluid and sufficiently flushed. Fluid sample was collected by opening and closing the valve with the ROV manipulator. Immediately after recovery of the ROV, sample bottles were incubated at 4 °C for 49–123 days until measurement in a shore-based laboratory. The bottles containing 4% formaldehyde were used as negative controls (i.e., with no microbial activity).

As a positive control for methane assimilation, stationary phase cells of a gammaproteobacterial methanotroph, *Methylomarinum vadi*, (Hirayama et al. 2013) were incubated in its medium (Hirayama et al. 2007) at 37 °C for 1 day under the same substrate condition (0.4 mM) as the

aerobic methanotrophic activity measurement, as described above. The cell density of *M. vadi* was adjusted to be  $2.0 \times 10^6$  cells in the bottle ( $1.3 \times 10^4$  cells/mL). As a positive control for bicarbonate assimilation, natural deep-sea diffusing hydrothermal fluid (average fluid temperature of 57 °C) from the Iheya North field (Takai et al. 2004), sampled in July–August 2010 using the same method described in previous sections of the present study, was incubated at 60 °C for 5 days under the same substrate condition (10 mM). The cell density of microbial community in the CORK fluid was  $1.0 \times 10^2$  cells/mL, thus each incubation bottle contained  $1.5 \times 10^4$  cells.

CORK fluid samples (approx. 150 mL) were incubated with radio-isotope-tracers for 49–123 days at 4 °C and then depressurized and filtered with a 0.22 µm-pore-sized cellulose acetate filters. Each filter was fixed with 10 mL of 4% (*w/v*) paraformaldehyde/PBS solution (pH 7.2) for 30 min, then thoroughly rinsed with filter-sterilized 0.1 M HCl in 3% (*w/v*) NaCl solution to remove carbonate precipitates. The filter was slurried in 20 mL of Hionic Flour cocktail (PerkinElmer, Waltham, MA, USA), and the radioactivity measured using a Tri Carb 2910TR liquid scintillation counter (PerkinElmer, Waltham, MA, USA). The assimilation rates of the tracers were calculated from concentrations and radio-isotope ratios given as the substrate in the initial state and the radio-isotope abundance of the filter. Blanks were evaluated by non-labeled batch incubation and used for calibration.

## Results

### pH, chlorinity, and major and minor ions

Concentrations of major and minor ions in the fluids were nearly identical in all samples, regardless of the sampling device used for collection (Additional file 1: Table S1). The chemistry of conservative components in CORK fluids were quite similar to those of deep (> 20 mbsf) porewater samples (DPW) obtained from the ODP Holes 1200 (Additional file 1: Table S1). For example, the fluid chlorinity (503–510 mmol/kg) of CORK fluids was distinguishable from seawater level (540 mmol/kg) and identical to those of the DPW ( $510 \pm 5$  mmol/kg) (Fig. 3a). CORK fluids ranged from 12.1 to 12.3 in pH values, which were slightly lower than the highest pH of  $12.5 \pm 0.1$  in the DPW (Fig. 3b). Slight differences between CORK fluids and the DPW in alkali metals (K, Li, Rb) (Additional file 1: Table S1) have been interpreted to be due to sampling artifacts during the core recovery and porewater extraction of the ODP serpentinite samples (de Lange et al. 1992; Wheat et al. 2008). Alkali earth metals (Mg, Ca, Sr) were depleted in the CORK fluids, as well as the DPWs (Fig. 3c). Seawater entrainment during the seafloor sampling cannot be evaluated precisely, because any entrainment of Mg from seawater would be precipitated immediately as

brucite. Nevertheless, the nearly identical and high concentrations of B, for example (Fig. 3d), are consistent with a scenario where mixing with ambient seawater during sample collection was minimal. Combined, these data are consistent with the CORK fluids being derived from a deep-sourced formation fluid that flowed into the borehole through screens located at a depth range of 149 and 202 mbsf.

### Sulfate, alkalinity, sulfide, and ammonium

Sulfate concentrations in the discharging CORK fluids were 0.4–1.7 mM, significantly lower than the concentration of 28 mmol/kg in the DPW and the seawater (Fig. 3e). The alkalinities of these fluids were much higher (119–126 meq/kg) than in the DPW (62 meq/kg) (Fig. 3f) and comparable to the value estimated from the previous CORK fluid observation (104 meq/kg) (Wheat et al. 2008). Both sulfate concentration and alkalinity in the CORK fluid from Dive #941 were in-between values of the DPW and other CORK fluids. These results point to a stoichiometry of 2 meq increase of alkalinity with 1 mmol decrease of sulfate in the CORK fluids when compared to the DPW (Fig. 4a). Dissolved reduced sulfur (sulfide) in CORK fluids was significant despite negligible sulfide concentrations detected in the DPW and showed a temporal decreasing trend: ~24 mM in 10 days, 21 mM in 4 months, and ~10 mM in more than 36 months (Fig. 3g). The sum of sulfate and sulfide concentrations in the CORK fluids were not higher than 28 mM, suggesting quantitative conversion in addition to the removal of dissolved sulfur to the solid phase (Fig. 4b). Ammonium concentrations were identical at 0.2–0.3 mM among all CORK fluids and the DPW (Additional file 1: Table S1). The highly variable alkalinity with the constantly low ammonium concentrations implies that the alkalinity variation do not result from the decomposition of sedimentary Redfield organic matter (Redfield, 1958) but from that of N-depleted organic carbon such as CH<sub>4</sub>.

### Gas composition and stable isotopes

Methane concentrations in the CORK fluids were variable between 5.5–6.1 mM in 10 days, 9.2–37.8 mM in 4 months, and 16.1–37.4 mM in more than 36 months after the valve was opened, respectively (Fig. 3h). CH<sub>4</sub> concentrations in CORK fluids were significantly higher than those observed in the DPW (< 2 mM). The differences strongly suggest that CH<sub>4</sub> was degassed from the DPW during core recovery and sample processing during the ODP Leg 195 (Mottl et al. 2003). This claim is consistent with a solubility-controlled CH<sub>4</sub> concentration of ~2 mM at room pressure and temperature (Wiesenburg and Guinasso jr, 1979). The CH<sub>4</sub> concentrations in CORK fluids are the highest among any deep-sea serpentinization-associated geofluid systems

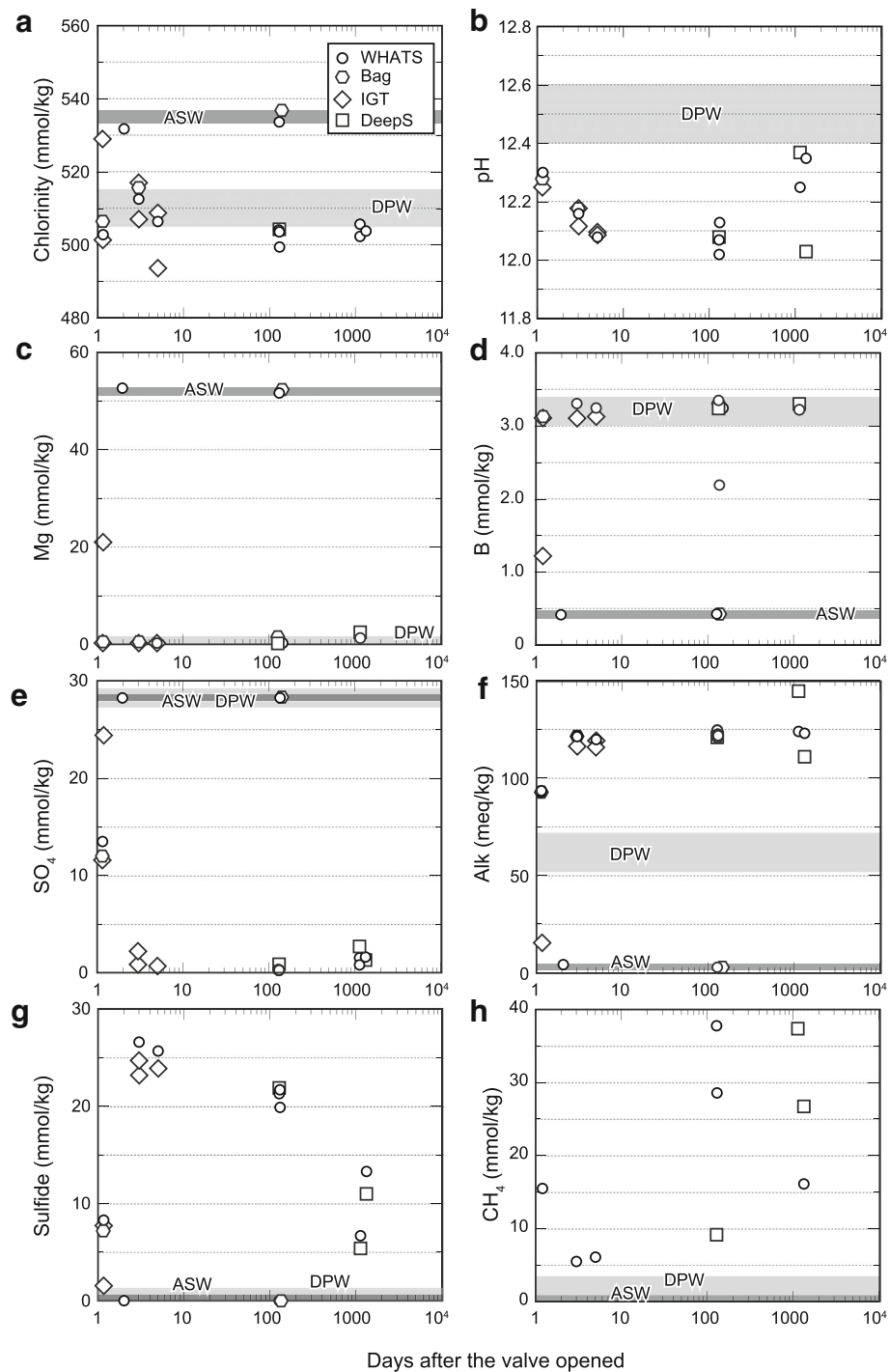


**Fig. 3** Time-series of fluid chemistry since the valve opening. Light and dark gray bars represent the deep part of the ODP porewater at Site 1200 (DPW) (Mottl et al. 2003) and ambient seawater (ASW) composition, respectively. Each symbol represents a type of fluid sampler used: WHATS (circle), Bag (hexagon), IGT (diamond), and Deep Sampler (square). Time (x axis) is in logarithmic scale

reported to date (<2 mM) (Charlou et al. 2002; Kumagai et al. 2008; Schrenk et al. 2013; Konn et al. 2015; McDermott et al. 2015; Seyfried et al. 2011). Ethane concentrations were also variable between 0.01 and 0.23 mM. Relative abundances of CH<sub>4</sub> to C<sub>2</sub>H<sub>6</sub> (C<sub>1</sub>/C<sub>2</sub>) were ~27 in 1 day,

216–3178 in 10 days to 4 months, and 231–285 in ~36 months after the valve opening. Molecular hydrogen concentrations in the CORK fluids ranged between 0.003 and 0.107 mM and were the lowest among values reported from deep-sea serpentinization-associated geofluid systems

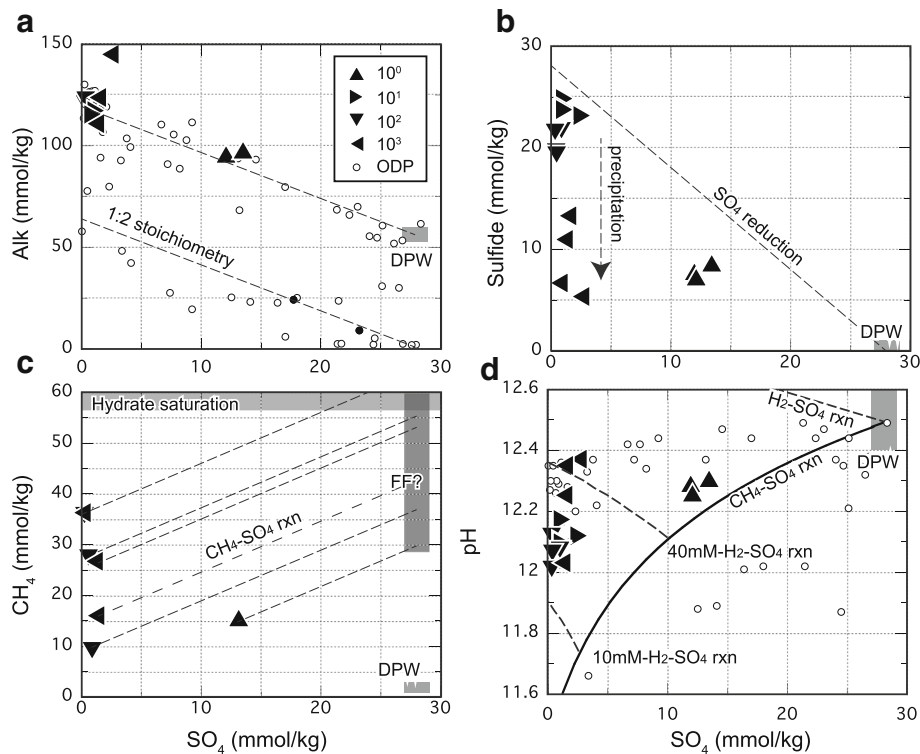


**Fig. 4** Relationships between sulfate and alkalinity, sulfide,  $\text{CH}_4$ , and pH. Filled triangles represent the CORK fluids from the present study, classified by the number of days after the valve was opened. Filled and open circles represent the CORK fluid observed in 2003 and DPW, respectively, shown for comparison. Filled gray zones represent the estimated endmember formation fluid composition of the ODP porewater (DPW) or a solubility of  $\text{CH}_4$  hydrate clathrate under the SCS condition (only shown in panel c). Broken lines in panels (a), (c), and (d) represent ideal changes in the chemical composition based on selected reactions. The dark gray zone in panel (c) represents possible  $\text{CH}_4$  concentrations of the SCS formation fluid (FF) without post-drilling alteration. The solid curve in panel (b) represents sulfate consumption through  $\text{CH}_4$ - $\text{SO}_4$  reaction from the porewater-based endmember. Broken curves in panel (b) represent sulfate consumption with 10, 40, and > 112 mM of  $\text{H}_2$ , in addition to the  $\text{CH}_4$ - $\text{SO}_4$  reaction

to date (> 1 mM) (Charlou et al. 2002; Kumagai et al. 2008; Schrenk et al. 2013; Konn et al. 2015; McDermott et al. 2015; Seyfried et al. 2011). Relative abundances of  $\text{CH}_4$  to  $\text{H}_2$  ( $\text{CH}_4/\text{H}_2$ ) ranged from 333 to 1350 for the CORK fluids. This  $\text{CH}_4/\text{H}_2$  ratio is higher than those of seafloor geofluids associated with serpentinization in other geologic settings (< 1). Total dissolved inorganic carbon (DIC), extracted and quantified as  $\text{CO}_2$ , ranged from 17 to 51 mM, which is consistent with the estimated carbonate alkalinity of the DPW (45 meq/kg; Mottl et al. 2003). The potentially insufficient acidification of DIC samples prior to the gas analysis may result in the underestimation of DIC concentrations in the CORK fluids.

Carbon and hydrogen isotopic ratios of methane ( $\delta^{13}\text{C}_{\text{C1}}$  and  $\delta\text{D}_{\text{C1}}$ ) and ethane ( $\delta^{13}\text{C}_{\text{C2}}$  and  $\delta\text{D}_{\text{C2}}$ ) were uniform among the CORK fluids, with values of  $-37\text{‰}$ ,  $-117\text{‰}$ ,  $-11\text{‰}$ , and  $-86\text{‰}$ , respectively, regardless of concentration (Additional file 1: Table S1). The  $\delta^{13}\text{C}_{\text{C1}}$  value of CORK fluids is significantly lower than other serpentinization-associated hydrothermal fluids reported to date (>  $-18\text{‰}$ ) (Fig. 5a) (Charlou et al. 2002; Kumagai

et al. 2008; Schrenk et al. 2013; Konn et al. 2015; McDermott et al. 2015). The higher  $\delta^{13}\text{C}_{\text{C1}}$  value in the shallow ODP porewater observed previously ( $-11 \pm 5\text{‰}$  at 15 mbsf; Mottl et al. 2003) is significantly different from the CORK fluid and is likely attributed to  $^{13}\text{C}$  enrichment in the remnant  $\text{CH}_4$  due to microbial methanotrophic activity in the fluid-seawater interface. The  $\delta^{13}\text{C}_{\text{C2}}$  value of the CORK fluids falls into the range of  $\delta^{13}\text{C}_{\text{C2}}$  values observed in serpentinization-associated hydrothermal fluids ( $-14\text{‰}$  to  $-2\text{‰}$ ) (Konn et al. 2015). The  $\delta\text{D}_{\text{C2}}$  value of the CORK fluids ( $-86\text{‰}$ ) is higher than that of the Lost City field ( $\sim -150\text{‰}$ ) (Fig. 5b). Total DIC of the CORK fluids showed  $\delta^{13}\text{C}_{\text{DIC}}$  values of  $-2.9\text{‰}$  to  $+1.4\text{‰}$ . The  $\delta^{13}\text{C}_{\text{DIC}}$  values close to  $+0\text{‰}$  suggest that the DIC originates from sedimentary carbonate ( $\sim +0\text{‰}$ ) rather than photosynthesis-based organic matter ( $\sim -25\text{‰}$ ) (Sano and Marty 1995). Hydrogen isotope ratios of  $\text{H}_2$  ( $\delta\text{D}_{\text{H2}}$ ) were  $-787\text{‰}$  to  $-761\text{‰}$ , which can be attributed to  $\text{H}_2$ - $\text{H}_2\text{O}$  hydrogen isotope equilibrium at an in situ temperature of  $2^\circ\text{C}$  (Horibe and Craig, 1995) when using the  $\delta\text{D}_{\text{H2O}}$  value of  $+12\text{‰}$  observed in the DPW (Mottl et al. 2003).

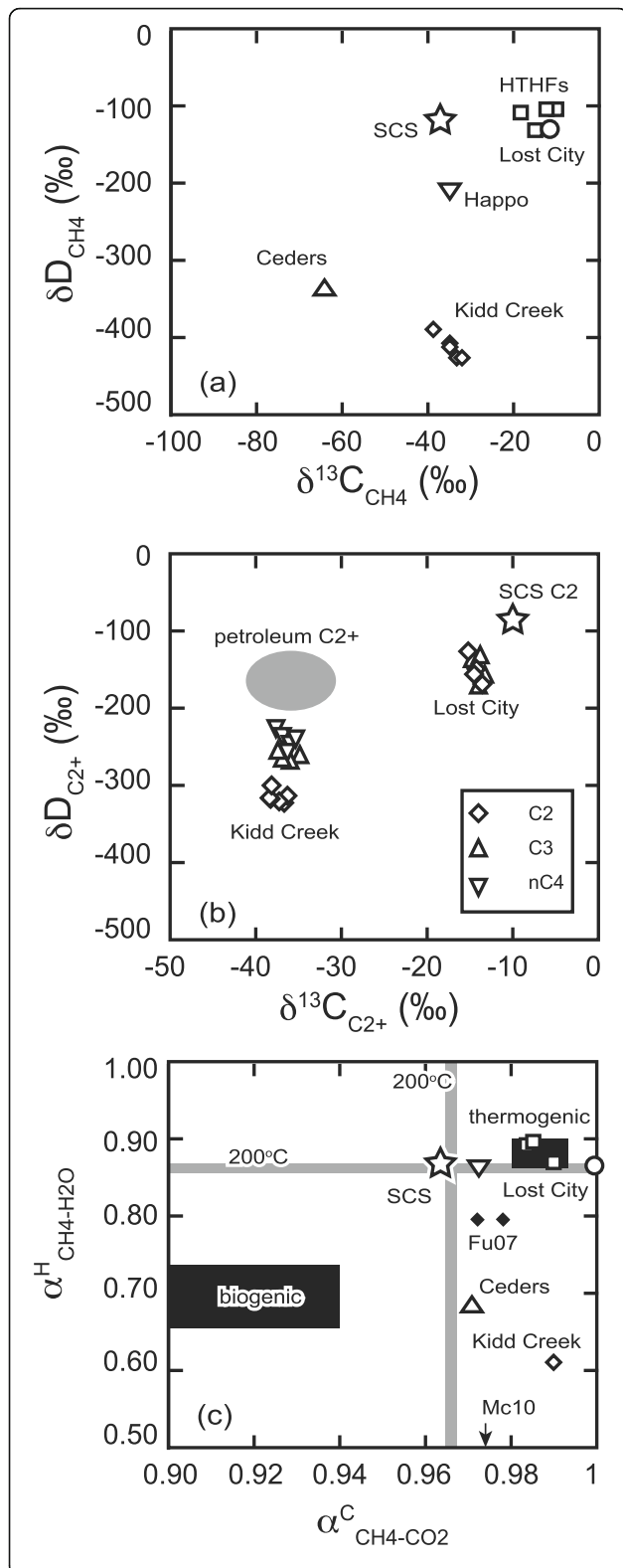


**Fig. 5** Stable isotope composition of CH<sub>4</sub>, C<sub>2</sub>H<sub>6</sub>, and the relevant molecules. Open and filled symbols, respectively, represent data from observations of hydrocarbon-enriched geofluid systems and experiments simulating methanogenesis. Data sources are following: high-temperature hydrothermal fluids (Konn et al. 2015; Kawagucci et al. 2016 and references therein), Lost City (Proskurowski et al. 2006; 2008), Haplo (Suda et al. 2014), The Ceders (Wang et al. 2015), Kidd Creek (Sherwood-Lollar et al. 2002), petroleum field (Burruss and Laughrey 2010), magnetite experiments (Fu et al. 2007), Fe experiment (McCullom et al. 2010), thermogenic experiment (Seewald et al. 1994) (assuming the CH<sub>4</sub>-H<sub>2</sub>O isotope equilibrium), and microbial incubation (Okumura et al. 2016b)

### Microbial cell density

Microbial cell densities of CORK fluids were estimated by epifluorescence microscopy (Table 2). In the blackish fluid discharging at the time when the valve was first opened (Dive #941), we measured a microbial cell density of  $2.0 \times 10^3$  cells/mL. This is much lower than the cell density in the ambient seawater ( $2.2 \times 10^4$  cells/mL) sampled during the same cruise (Table 2). The microbial cell densities in the clear CORK fluid sampled 4 days and 4 months after the valve opening decreased to  $4.4\text{--}6.6 \times 10^2$  and  $1.0 \times 10^2$  cells/mL, respectively (Table 2). These results suggest that, before the valve opening, certain microbial communities maintained their populations and functions in some of the microhabitats in the stagnant CORK fluid of the sealed borehole and well-head structures. Such local microbial populations in the stagnant fluid system were flushed out by the newly created discharging fluid flow after the valve was opened. After more than 36 months, however, the microbial cell densities in the CORK fluid were  $4.1\text{--}7.6 \times 10^3$  cells/mL (Table 2).

### Microbial phylotype compositions

The 16S rRNA gene phylotype compositions of microbial communities in CORK fluid samples at the time that the valve was opened, 3 days later, and 45 months later were examined. In total 89, 88, and 44 clones were sequenced for the microbial communities in the CORK fluid samples at the time of valve opening, 3 days later, and 45 months later, respectively (Fig. 6). The phylotype compositions were significantly different among the fluid samples.

In the blackish discharging fluid ( $2.0 \times 10^3$  cells/mL of microbial cell density), the gamma-proteobacterial phylotypes dominated the clone library and consisted almost entirely of a single phylotype closely related with *Methylobactor*, a methanotrophic endosymbiont of *Bathymodiolus* mussels living in the SCS seepage sites (Fig. 6). The alpha-proteobacterial and actinobacterial phylotypes were the second most abundant groups in the library. Other components were phylotypes of *Betaproteobacteria* and *Firmicutes*. In the

**Table 2** Microbial cell density in the CORK fluid and ambient seawater samples

Cruise ID	HPD dive#	Time after valve opening	Sample type	Cell count (cells ml <sup>-1</sup> )
NT09-01	941	0 day	Bag	2000
NT09-01	943	2 days	Bag	440
	943	(ambient seawater)	Bag	22,000
	945	4 days	Bag	660
	1007	5 months	Bag	101
NT09-07	1009	5 months	Bag	139
	1349	45 months	WHATS	7600
NT12-04	1350	45 months	Deep sampler	4100

CORK fluid obtained 3 days after opening ( $4.4\text{--}6.0 \times 10^2$  cells/mL of microbial cell density), the gamma-proteobacterial phylotypes, especially the *Methylobactor* phylotype, significantly decreased in the relative abundance and alpha-proteobacterial phylotypes also decreased in the relative clonal abundances (Fig. 6). In contrast, phylotypes of *Deltaproteobacteria*, *Firmicutes* (*Alkaliphilius*), *Actinobacteria*, *Deinococcus-Thermus*, and *Archaea* increased in relative abundances. Most archaeal phylotypes were related to extremophilic members such as hyperthermophiles and extreme halophiles that do not inhabit the cold and highly alkaline serpentine formation fluid regime of the SCS (Fig. 6). Although this simplified interpretation may lead to misunderstanding since the microbial cell density was decreased by

fluid replacement during the 3-day discharge of the CORK fluid, phylotypes that increased in clonal abundances 3 days after the valve opening more likely represent truly indigenous microbial populations entrained by the serpentinite formation fluid derived from the deep. In the CORK fluid obtained by the Deep Sampler 45 months after the valve opening ( $4.1\text{--}7.6 \times 10^3$  cells/mL of microbial cell density), the microbial phylotype composition changed drastically (Fig. 6). Most of the predominant phylotypes found in the fluids were different from those sampled 3 days after the valve was opened. At 45 months after, phylotypes of *Deltaproteobacteria*, *Epsilonbacteria*, *Planctomycetes*, *Thermus-Deinococcus*, and unclassified bacterial group dominated the library. It is still unclear why the CORK fluid obtained by the

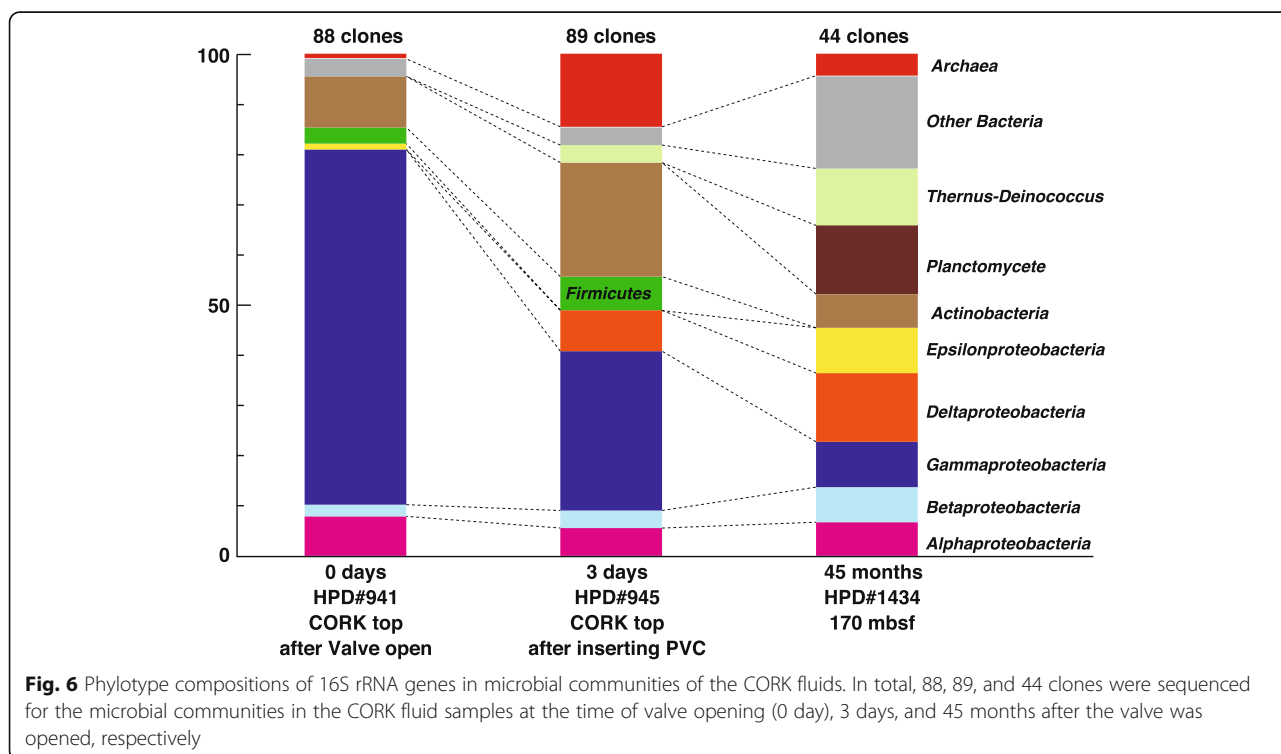


**Fig. 6** Phylotype compositions of 16S rRNA genes in microbial communities of the CORK fluids. In total, 88, 89, and 44 clones were sequenced for the microbial communities in the CORK fluid samples at the time of valve opening (0 day), 3 days, and 45 months after the valve was opened, respectively

Deep Sampler 45 months after had a higher cell density and a different microbial phylotype composition compared to the initial phase of CORK fluids. Nevertheless, it should be noted that the sampling scheme by the Deep Sampler was different from those by other fluid samplers, with the Deep Sampler (5 cm in diameter with the bottle being 1 m in length) was delivered to 170 mbsf through the cased borehole. During the descent, the bottle could have hit the casing wall and detached accreted materials which likely contain microbial populations. Thus, the microbial community abundance and composition in the fluid obtained by the Deep Sampler may include, in addition to the microbial communities entrained from the formation fluid (“pelagic”) flow, microbial populations specifically colonizing the steel casing pipe wall (Nakagawa et al. 2006; Nigro et al. 2012).

### Microbial carbon assimilation activity

Microbial methane-, carbon monoxide-, formate-, acetate-, and leucine-assimilations (methanotrophic, carboxydrotrophic, and heterotrophic activities) were examined with the CORK fluid samples obtained 1 to 6 days after the valve opening, and the bicarbonate-, methane-, formate-, and acetate-assimilation activities were examined with the CORK fluid samples obtained 5 months after the valve opening (Table 3). *Methylomarinum vadi* is a marine aerobic methanotroph optimally growing at 37 °C with a generation time of 2 h (Hirayama et al. 2013), and the methane assimilation rate of this methanotroph under the maintenance state for 1-day incubation was used as the positive control: 20 nmol/day/L with a cell density of  $1.3 \times 10^4$  cells/mL (Table 3). In a similar manner, the autotrophic bicarbonate assimilation of natural deep-sea diffusing hydrothermal fluid was determined to be 2.3 nmol/day/L with a cell density of  $1.0 \times 10^2$  cells/mL (Table 3).

These methane assimilation rates of *M. vadi* and the bicarbonate assimilation of the natural autotrophic microbial community in the discharging fluid are good comparative indexes to estimate the functions of the methanotrophic and autotrophic populations and even the whole microbial community in the CORK fluid.

The methane assimilation rates were determined to be 0.036, 0.049 and 0.039 nmol/day/L in the CORK fluid under in situ, microaerobic and fully anaerobic conditions, respectively (Table 3). These values were significantly higher than those of the negative controls with the same tracers and are attributed to activity from the microbial populations in the CORK fluid. In addition, these values correspond to the methane assimilation activity by  $2.3\text{--}3.2 \times 10^1$  cells/mL through aerobic methanotrophy in the maintenance state. Carbon monoxide assimilation was not detected, while heterotrophic carbon assimilation was found to be the highest with formate (0.06 nmol/day/L) and the lowest with acetate (0.004 nmol/day/L). These values are similar to or lower than the methane assimilation activity. In the CORK fluid obtained 5 months after the valve opening, autotrophic bicarbonate assimilation activity was the highest (1.4 nmol/day/L), and methanotrophic and heterotrophic (with formate and acetate) assimilations were lower at 0.2 and 0.05 nmol/day/L, respectively (Table 3). The methanotrophic assimilation was higher than any of the methane assimilation activities using the CORK fluid obtained 1 to 6 days after valve opening and the heterotrophic activity was similar to values reported previously from the CORK fluid, although the cell density in the CORK fluid decreased from  $4.4\text{--}6.6 \times 10^2$  to  $1.0 \times 10^2$  cells/mL during the 5 months period. Compared to the values of positive controls, these autotrophic and methanotrophic assimilation activities correspond to  $7.0 \times 10^1$  cells/mL of a natural autotrophic microbial

**Table 3** Radio-isotope-tracer carbon assimilation of microbial community in the CORK fluids and positive controls

Cruise ID	HPD dive#	Tracer and incubation condition	Incubation time (days)	Net assimilation (nmol day <sup>-1</sup> L <sup>-1</sup> )
NT09-01	943	<sup>14</sup> C-CH <sub>4</sub> (0.25 MBq per bottle and 0.4 mM)	54	0.036
	943	<sup>14</sup> C-CH <sub>4</sub> (0.25 MBq per bottle and 0.4 mM) with 40 μM O <sub>2</sub>	54	0.049
NT09-01	947	<sup>14</sup> C-Leucine (0.25 MBq per bottle and 0.1 mM)	52	0.014
	947	<sup>14</sup> C-Formate (0.25 MBq per bottle and 0.1 mM)	52	0.06
	947	<sup>14</sup> C-Acetate (0.25 MBq per bottle and 0.1 mM)	52	0.004
NT09-01	948	<sup>14</sup> C-CH <sub>4</sub> (0.25 MBq per bottle and 0.4 mM) with 10 mM NaSO <sub>4</sub> and 0.5 mM Na <sub>2</sub> S	49	0.039
	948	<sup>14</sup> C-CO (0.25 MBq per bottle and 0.4 mM)	49	n.d. <sup>a</sup>
NT09-07	1007	<sup>14</sup> C-CH <sub>4</sub> (0.25 MBq per bottle and 0.4 mM)	123	0.2
	1007	<sup>14</sup> C-HCO <sub>3</sub> <sup>-</sup> (0.25 MBq per bottle and 0.1 mM) with 0.4 mM H <sub>2</sub>	123	1.4
	1009	<sup>14</sup> C-Formate and <sup>14</sup> C-acetate (each of 0.25 MBq per bottle and 0.1 mM)	122	0.05
An aerobic methanotroph culture		<sup>14</sup> C-CH <sub>4</sub> (0.25 MBq per bottle and 0.4 mM)	1	20
An autotrophic community in diffusing hydrothermal fluid		<sup>14</sup> C-HCO <sub>3</sub> <sup>-</sup> (0.25 MBq per bottle and 0.1 mM)	5	2.3

<sup>a</sup>n.d. not detected

community and  $1.3 \times 10^2$  cells/mL of relatively inactive aerobic methanotrophs. These results indicate that the small number of microbial cells present in the CORK fluid obtained 5 months post-valve opening may be functionally active and capable of methanotrophic and autotrophic metabolisms. Nevertheless, radio-isotope-tracer experiments clearly indicate that microbial metabolisms and activities in the CORK fluids are detectable.

## Discussion

### Post-drilling fluid alteration

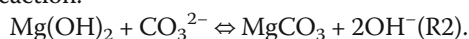
#### *Sulfate reduction coupled with CH<sub>4</sub> oxidation*

Except for sulfate, the consistency in the major ion fluid chemistry between the CORK fluid and the DPW suggests that CORK fluids originate from the deep SCS formation fluid. Sulfate depletions in the CORK fluids, as opposed to the sulfate enrichment seen in the DPW, likely resulted from perturbation of the seafloor geochemical environment during drilling activity. To estimate the abundance of reactive components (particularly CH<sub>4</sub> and H<sub>2</sub>) in the pristine SCS formation fluid, it is necessary to consider processes associated with the drilling operation that could alter the fluid chemistry at  $\sim 4$  °C.

A previous study (Wheat et al. 2008) pointed out that the methane oxidation can cause SO<sub>4</sub> depletion in the CORK fluid, as follows:



R1 produces 1 mol of dissolved sulfide and two equivalents of alkalinity for each mole of OH<sup>-</sup>, CH<sub>4</sub>, and SO<sub>4</sub><sup>2-</sup> consumed. This stoichiometry is consistent with the stoichiometry exhibited by the differences between the DPW and CORK fluids (Figs. 3 and 4). Assuming that R1 fully accounts for the  $\sim 27$  mM-equivalent sulfate consumption in the CORK fluids, the pristine SCS formation fluids would have contained CH<sub>4</sub> at concentrations of 35–65 mM (Fig. 4c). The measured pH values of the CORK fluids (12.1–12.3) were higher than would be expected given the consumption of  $\sim 27$  mM OH<sup>-</sup> and a DPW with a pH = 12.5  $\pm$  0.1 that is representative of the SCS formation fluid (Fig. 4d). In addition, some of the measured total DIC contents of the CORK fluids (17–51 mM) were also inconsistent with a DIC concentration of  $\sim 50$  mM expected by a combination of the  $\sim 27$  mM DIC production and the 23 mM DIC being originally present in the pristine SCS formation fluid (Mottl et al. 2003). Differences in the OH<sup>-</sup> and DIC values between the measured and predicted fluid compositions may be due to brucite-magnesite buffer through the following reaction:

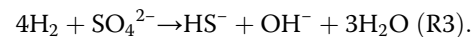


The maximum CH<sub>4</sub> concentration estimated (65 mM) seems too high but is not unrealistic because it is comparable to the solubility of CH<sub>4</sub> clathrate hydrate under

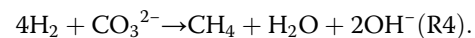
relevant concentration-pressure-temperature-salinity condition within the SCS ( $\sim 60$  mM at 30 MPa, 2 °C and 3.5%) (Tishchenko et al. 2005). No geophysical data, however, support the presence of layered hydrate boundary, such as bottom simulating reflector (BSR).

#### *Possible H<sub>2</sub> consumption coupled with sulfate reduction*

The low concentrations of H<sub>2</sub> in the CORK fluid ( $< 0.1$  mM) suggest that it may be consumed by sulfate reduction in addition to CH<sub>4</sub>. H<sub>2</sub> oxidation coupled with sulfate reduction progresses as follows:



Because R3 produces OH<sup>-</sup>, H<sub>2</sub> consumption during sulfate reduction may contribute to measured pH values that are higher than predicted by R1 (Fig. 4d). Assuming the pH balance is made by R1 and R3, the native SCS formation fluid may contain as much as  $\sim 40$  mM of H<sub>2</sub>. This H<sub>2</sub> level may be realistic because 27 mM of H<sub>2</sub> has been observed in a seafloor serpentinization-associated hydrothermal system at  $> 296$  °C (Konn et al. 2015) and  $> 100$  mM of H<sub>2</sub> can be attained through serpentinization at 200–300 °C from thermodynamic calculation (McCollom and Bach 2009). If the cool SCS formation fluid contains such abundant H<sub>2</sub>, the reduction of CO<sub>2</sub> to form CH<sub>4</sub> is thermodynamically favorable, according to the following reaction:



However, abiotic CH<sub>4</sub> formation represented by R4 is unlikely due to kinetic barriers at the low temperatures within the SCS body (4 °C). In addition to CH<sub>4</sub> and H<sub>2</sub>, native iron and other metals in the casing pipe may function as reductant and cation for the dissolved sulfate removal.

#### *Drilling induced sulfate reduction*

The discussions above suggest that abundant CH<sub>4</sub> and SO<sub>4</sub> coexist in the native SCS formation fluid and is consistent with their presence in the DPW (Mottl et al. 2003). This coexistence is unusual in the seafloor environment because sulfate reduction coupled with methane oxidation is thermodynamically favorable and usually promoted by ubiquitous microbial consortia of methanotrophic archaea and sulfate reducing bacteria, known as AOM (Orphan et al. 2001). In other words, both abundant CH<sub>4</sub> and SO<sub>4</sub> in the native SCS formation fluid point to unusually slow kinetics of the sulfate reduction (R1) within the native SCS body. In fact, SO<sub>4</sub> reduction coupled with CH<sub>4</sub> oxidation (R1) likely occurs in the post-drilling CORK fluids, derived from

subseafloor regions affected by the Hole 1200C drilling, casing, and/or CORK installation.

Drilling-induced introduction of external microbial communities into the subsurface environment may account for the post-drilling progression of R1 due to AOM. While the relatively impermeable serpentinite matrix prevented access of the over-pressured aquifer to the microbe-bearing seawater, the drilling operation and the hole made the deep aquifer exposed to deep-sea water and shallow subseafloor sediment containing exogenous microbial communities, including AOM consortia (Mottl et al. 2003). However, the post-drilling microbial AOM function is likely insignificant, as suggested by multiple lines of microbiological evidence such as small biomass, a lack of evidence for 16S rRNA gene phylotype signatures of previously known AOM consortia, and the negligible  $\text{CH}_4$  assimilation during the  $^{14}\text{C}$  experiment (see the “Results” section). Assuming that the dissimilatory AOM activity of consortia does not exceed  $10^2$  times higher than the anoxic methane assimilation rate, as the highest methane assimilation activity estimated in this study is  $0.0002 \mu\text{mol/day/L}$ , it can be calculated that a  $27 \text{ mmol/L SO}_4$  consumption requires  $> 10^6$  days. This amount of time is much longer than the time elapsed since drilling ceased ( $< 10^4$  days). This calculation, together with other microbiological results, suggests that the microbial AOM function is not significantly involved in the post-drilling  $\text{CH}_4$ - $\text{SO}_4$  reactions, based on experimental conditions at  $2 \text{ }^\circ\text{C}$ . Although faster microbial reaction rates may occur deeper within the seamount where the environment is warmer, the extent of their involvement would be still negligible. It is noted that microbial activity at the pristine interior of the SCS body is more strictly limited than the rate calculated above due to their impermeability and over-pressured aquifer, and probably less biomass.

There are no reliable data for the kinetics of R1 without the involvement of microbial AOM. However, the sudden and rapid progression of R1 after drilling would require some catalytic effects associated with the drilling, casing, and CORK installation operations, other than the introduction of AOM populations. A possible catalyst introduced by drilling and casing the borehole is native iron and other metals used in the casing pipe and the CORK structure. Transition metals such as iron and nickel generally exhibit catalytic function for redox reactions due to their multiple valences. In addition to catalytic reactions occurring locally on the metal surface, high electron conductivity of the elongate casing pipe allows remotely located reducing and oxidizing molecules to be reacted through electron transfer, similar to how a battery functions. Nevertheless, the extent to which drilling and casing operations promoted abiotic sulfate reduction coupled with  $\text{CH}_4$  oxidation is still not entirely clear.

### Origins of $\text{CH}_4$ and $\text{SO}_4$ in the native serpentinite formation fluid of the SCS

#### *Abiotic hydrocarbon synthesis associated with serpentinitization—environmental factors*

Although it is difficult in natural environments of the modern Earth to distinguish between abiotic synthesis of  $\text{CH}_4$  from other  $\text{CH}_4$  sources such as microbial methanogenesis (biogenic  $\text{CH}_4$ ) and thermal degradation of sedimentary organic matter (thermogenic  $\text{CH}_4$ ) (see reviews, Etiope and Sherwood Lollar, 2013 for example), multiple lines of geochemical and microbiological evidence suggest that contributions of biogenic and thermogenic  $\text{CH}_4$  in the SCS system are not significant. During the early stage of subduction, where the temperatures are below the known  $122 \text{ }^\circ\text{C}$  upper limit for the growth of microbes (Takai et al. 2008), microbial methanogenesis is probably absent or insignificant due to the abundantly dissolved sulfate in the sediment pore water in the Pacific plate eastward from the Mariana Trench (ODP sites 800–802) (France-Lanord et al. 1992). During the later stages of subduction, temperatures exceed  $122 \text{ }^\circ\text{C}$ , which is too high for microbial life to survive. The same is also true for regions of extensive serpentinitization within the overlying mantle wedge. In the SCS formation fluid regime, where temperatures again become cool and habitable, there is little potential to produce abundant  $\text{CH}_4$  due to low biomass and microbial function, revealed by the 45 months long observation of the CORK fluids. In addition, the highest known pH limit for the growth of methanogens is  $< 10$  (*Methanosalsum zhilinae*: Mathrani et al. 1988), significantly lower than the pH of  $> 12$  in the SCS fluids. The extremely low organic contents in the SCS serpentinite mud (Mottl et al. 2003) indicate that there is little potential for thermogenic hydrocarbon generation beneath the SCS.

#### **Possibility of abiotic synthesis from thermodynamic and kinetic viewpoints**

Abiotic organic synthesis, including the generation of  $\text{CH}_4$  from  $\text{CO}_2$ , is generally more favorable at lower temperatures from a thermodynamic viewpoint despite unfavorable kinetic constraints (e.g., McCollom, 2008). In the case of the SCS, thermodynamically favorable conditions for the abiotic synthesis of  $\text{CH}_4$  is expected through the entire formation fluid regime due to sufficiently reducing conditions resulting from serpentinitization occur at  $200\text{--}300 \text{ }^\circ\text{C}$  (McCollom and Bach, 2009) and subsequent cooled as fluids ascend. The ascending fluid is quenched sufficiently for microbial activity ( $122 \text{ }^\circ\text{C}$ : Takai et al. 2008) at  $13 \text{ km}$  below the seafloor, estimated from the thermal gradient observed ( $9.4 \text{ }^\circ\text{C/km}$ ). Since formation fluids probably ascend on a geological time span, continuous abiotic synthesis and accumulation of organic compounds is plausible, even at extremely low reaction rates.

The rate of abiotic hydrocarbon synthesis depends on the carbon substrate (McCullom et al. 2010). McCullom et al. (2010) demonstrated that CO-based synthesis is feasible within an experimental timeframe. Even when the CO-based abiotic synthesis is feasible under conditions of the SCS formation fluid, CO production from CO<sub>2</sub> represents a bottle-neck in the process due to the several orders of magnitude less CO compared to CO<sub>2</sub> in the CORK fluid. Abiotic methanogenesis based on solid-phase carbon, such as graphite derived from metamorphism and carbonate mineral deposits (Etioppe and Sherwood Lollar, 2013), cannot be precluded, although the possibility cannot be evaluated here due to limited information about the rates of such processes.

**Suggestions from stable isotope signatures** Stable isotope signatures should be interpreted in the context of isotope ratios of individual molecules (Fig. 5a, b) and isotope fractionation between relevant molecules (Fig. 5c) (Etioppe and Sherwood Lollar, 2013). The CH<sub>4</sub>-H<sub>2</sub>O hydrogen isotopic fractionation factor of the CORK fluid ( $\alpha^{\text{H}}_{\text{CH}_4\text{-H}_2\text{O}}$ ) is 0.87, which is inconsistent with typical biogenic values of  $\sim 0.70$  (Okumura et al. 2016b) (Fig. 5c). Thermogenic CH<sub>4</sub> reservoirs generally have  $\alpha^{\text{H}}_{\text{CH}_4\text{-H}_2\text{O}}$  values corresponding to the CH<sub>4</sub>-H<sub>2</sub>O isotope equilibrium values at the formation/reservoir temperature (e.g., Stolper et al. 2014; Wang et al. 2015). The  $\alpha^{\text{H}}_{\text{CH}_4\text{-H}_2\text{O}}$  and  $\alpha^{\text{H}}_{\text{C}_2\text{H}_6\text{-H}_2\text{O}}$  values of the CORK fluids ( $> 0.86$ ) correspond to those of the isotope equilibrium values at  $> 200$  °C (Fig. 5b, c) (Horibe and Craig 1995; Reeves et al. 2012), consistent with the uppermost temperature expected at the plate boundary and mantle wedge beneath the SCS ( $\sim 350$  °C) (Mottl et al. 2004; Hulme et al. 2010). This suggests that the hydrogen isotope signature of hydrocarbons recorded at  $> 200$  °C has not been altered after these fluids have been cooled to their discharge temperatures. The lack of hydrogen isotope re-equilibrium between CH<sub>4</sub> and H<sub>2</sub>O seems consistent with the half-life for equilibrium exchange, estimated to be approximately one million years at 200 °C (Sessions et al. 2004; Wang et al. 2015). In addition, the hydrogen isotope signature shows no evidence for a contribution of biogenic CH<sub>4</sub> produced in the cool formation fluid regime of the SCS. The H<sub>2</sub>-H<sub>2</sub>O thermometer value, indicating  $\sim 2$  °C, is inconsistent with the CH<sub>4</sub>-H<sub>2</sub>O thermometer but reasonable because of the more feasible H<sub>2</sub>-H<sub>2</sub>O equilibrium, even at lower temperatures (Valentine et al. 2004; Proskurowski et al. 2008; Kawagucci et al. 2010; 2016; Pester et al. 2018).

The  $\delta^{13}\text{C-CH}_4$  values of about  $-37\text{‰}$  and the isotope fractionation between CH<sub>4</sub>-DIC ( $\alpha^{\text{C}}_{\text{CH}_4\text{-DIC}}$ ) of  $\sim 0.963$  seem to be an equivocal signature for thermogenic, biogenic, or abiotic origins (Fig. 5c) (Kawagucci et al. 2013 and references therein). Hydrothermal experiments

simulating hydrothermal hydrocarbons generation from the seafloor sediment at 325–400 °C show an  $\alpha^{\text{C}}_{\text{CH}_4\text{-CO}_2}$  as high as 0.985 (Seewald et al. 1994) (Fig. 5c). Carbon isotope fractionation produced by microbial hydrogenotrophic methanogenesis in the seafloor sediment typically displays  $\alpha^{\text{C}}_{\text{CH}_4\text{-DIC}}$  of  $\sim 0.930$  (Okumura et al. 2016b and references therein). It is also known, however, that microbial metabolisms sometimes cause unusual isotope effects under extreme growth and survival conditions (e.g., Valentine et al. 2004; Penning et al. 2005; Takai et al. 2008). Microbial methanogenesis in the SCS formation fluid regime may cause an unusual carbon isotope effect as CO<sub>3</sub><sup>2-</sup> is the dominant DIC speciation in highly alkaline solutions.

Carbon and hydrogen isotope systematics of CORK fluids suggest that abiotic methanogenesis is occurring at  $> \sim 200$  °C. Hydrothermal experiments, demonstrating CO- and CO<sub>2</sub>-based abiotic hydrocarbon syntheses, provide consistent  $\alpha^{\text{C}}_{\text{CH}_4\text{-CO}_2}$  values of 0.97–0.98 (Fu et al. 2007; McCullom et al. 2010), slightly higher than that observed in the CORK fluids (0.963). Experimental determination of CH<sub>4</sub>-CO<sub>2</sub> isotope equilibrium at 200 °C exhibits a  $\alpha^{\text{C}}_{\text{CH}_4\text{-CO}_2}$  of 0.966 (Horita, 2001), very close to the value observed from the CORK fluid (Fig. 5c). Although carbon isotope exchange between CH<sub>4</sub>-CO<sub>2</sub> below  $\sim 400$  °C is generally thought to become kinetically sluggish without a catalyst, particularly in the CH<sub>4</sub>-generating direction (e.g., McCullom, 2008), the CH<sub>4</sub>-CO<sub>2</sub> isotope equilibrium could be attained at  $\sim 200$  °C beneath the SCS because of thermodynamically favorable condition for CH<sub>4</sub> generation and geological time span. For the hydrogen isotope equilibrium between hydrocarbons and H<sub>2</sub>O, terminal locality of hydrogen atoms would be more feasible for the exchange with the surrounding hydrogen-bearing molecules, namely, H<sub>2</sub>O (Reeves et al. 2012; Wang et al. 2015). The H exchange would erase the extremely D-depleted signature ( $\alpha^{\text{H}}_{\text{CH}_4\text{-H}_2\text{O}} = \sim 0.45$ ; McCullom et al. 2010) exhibited by the (experimental) abiotic CH<sub>4</sub> generation. Carbon and hydrogen isotopic thermometers both indicating  $> \sim 200$  °C left in the 2 °C CORK fluid (Fig. 5c), imply that the reactions for isotope exchange are limited at lower temperatures. Thus, the rate of abiotic synthesis would decrease after cooling the SCS formation fluid below 200 °C, yet it must continue within the serpentinite matrix at lower temperatures.

#### **Slab-derived SO<sub>4</sub> conservation through serpentinization**

The abundant dissolved sulfate in the SCS formation fluid was thought to originate from sulfate in the subducting slab (Mottl et al. 2003). This conclusion seems inconsistent with abiotic organic synthesis via serpentinization, in which sulfate should be reduced from a thermodynamic viewpoint. On the other hand, closed-system experiments

simulating serpentinization at 200–300 °C (Janecky and Seyfried Jr., 1986; Seyfried 2007) confirmed barriers to sulfate reduction during serpentinization due to rapid sulfate precipitation as anhydrite upon initial heating of the experiment and its subsequent metastable persistence, even in a highly reducing fluid. Accordingly, anhydrite precipitation in the downgoing slab may facilitate sulfate conservation through high-temperature regions of subduction and diapir. In addition, a recent quadruple sulfur isotope study of SCS DPW and CORK fluid suggests that the mantle wedge represents one of the possible sources of sulfate in the SCS formation fluid (Aoyama et al. 2018).

**Hypothetical sequence of geochemical processes in the SCS system**

We propose a hypothesis for the possible sequence of (bio) geochemical processes in the SCS serpentinite formation fluid regime, based on CORK fluid characteristics and observations from previous studies (Fig. 7). The oligotrophic western North Pacific water provides little sedimentary organic matter, resulting in pelagic sediments of the Pacific plate eastward from the Mariana

Trench (ODP sites 800–802) that contain sulfate-rich porewater (France-Lanord et al. 1992; Alt and Shanks III, 2006) and low sedimentary biomass (Kellmeyer et al., 2012). Global seafloor drilling that penetrates into the upper basaltic crust (e.g., Gieskes et al. 1990, 1993; Hensen and Wallmann, 2005) have indeed revealed dissolved sulfate that is ubiquitously abundant in the uppermost part of subducting plate, despite their great depth and distance from the trench seafloor. At an early stage of subduction, some or all of the porewater sulfate is precipitated as anhydrite with requisite Ca supplied by dissolution of sedimentary calcite or reactions with involving basaltic crust. At the deep plate boundary region at ~ 0.6 GPa and ≤ ~ 350 °C (Hulme et al. 2010), metamorphic processes such as compactive dewatering, expulsion of interlayer water, dehydration, and decarbonation forms the DIC-rich initial upwelling fluid (Mottl et al. 2004), which harbors no microbial population due to its high temperature. The initial fluid accompanied with metamorphic minerals such as blueschist and anhydrite penetrates into the overlying mantle wedge and induces serpentinization. Extensive serpentinization produces highly alkaline and strongly reducing H<sub>2</sub>-rich fluid

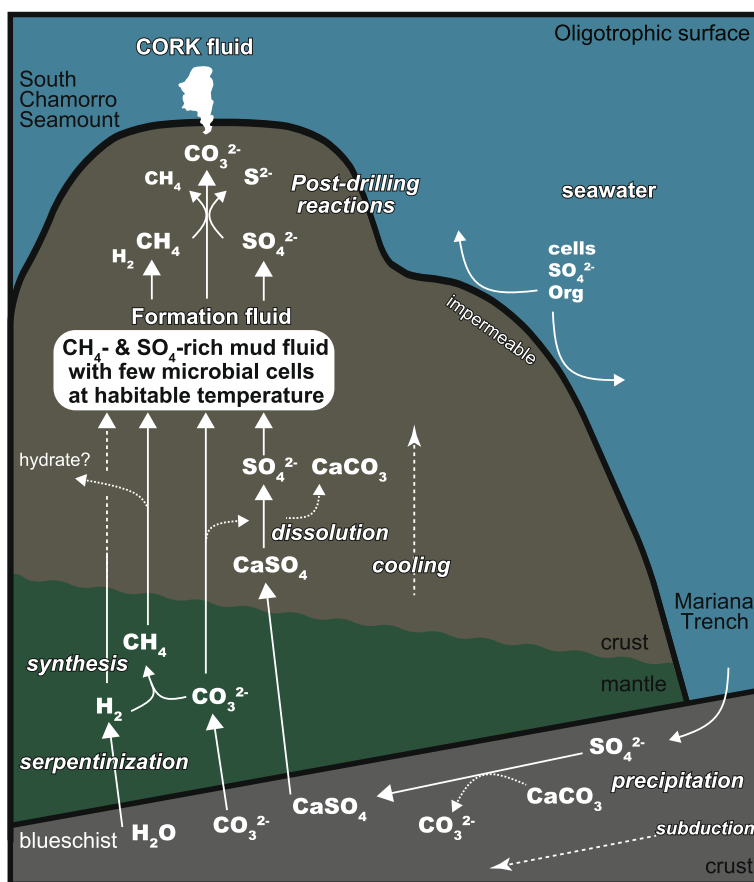


**Fig. 7** Illustration for possible C-S-H reactions beneath the SCS. “Cells” represents microbial cells and “Org” represents organic matter in the seawater

(McCollom and Bach 2009), leading to the thermodynamic conditions favorable for the abiotic organic synthesis from slab-derived inorganic carbon. Sulfate minerals are not reduced, due to kinetic constraints. The abiotic synthesis of organic molecules occurs within the ascending serpentinite mud until its temperature decreases to  $\sim 200$  °C. Further ascend and cooling decrease the rate of abiotic synthesis while allowing for the dissolution of anhydrite (anhydrite-derived calcium is completely removed by abundant DIC). This sequence results in the co-existence of abiotic  $\text{CH}_4$  (and possibly  $\text{H}_2$ ,  $\text{C}_{2+}$  hydrocarbons, and some organic matter) and slab-derived dissolved  $\text{SO}_4$  in the SCS formation fluid. Although the abundant  $\text{CH}_4$  and  $\text{SO}_4$  exhibit sufficient bioavailable energy potentials (Nakamura and Takai 2014) within the habitable temperature range ( $< \sim 122$  °C; Takai et al. 2008), limited microbial biomass and activity are present because the relatively impermeable SCS prevents penetration of microbial community from ambient seawater. As the major conduit for the mud/fluid ascending path consists of 60–100% serpentinite muds (Shipboard Sci. Party 2002), the fluid-serpentinite interaction rather than fluid-peridotite interaction (serpentinization) dominates the current fluid chemistry of the SCS formation fluid. The highly alkaline porewater pH of  $\sim 12.5$  likely prevents the development of seafloor microbial community due to the  $\text{CO}_3^{2-}$ -dominated DIC speciation being disadvantageous for autotrophy (e.g., Schrenk et al. 2013) whereas the known upper pH limit for chemoorganotrophic microorganisms is 12.4 (Takai et al. 2001). Ongoing reactions between the  $\text{CH}_4$  and  $\text{SO}_4$ , as observed in this study, would have been triggered by the very recent ODP drilling and casing operations carried out in 2001 (Shipboard Sci. Party 2002; Wheat et al. 2008).

## Conclusions

The present study investigated the chemical and microbiological characteristics of formation fluids from a serpentinite mud volcano, the SCS. The gas chemistry characterized by abundant  $\text{CH}_4$  and low  $\text{H}_2$  is the first of its kind from deep-sea highly alkaline (serpentinization-associated) geofluid systems. The SCS formation fluid regime may also represent the first reported example on Earth where abiotic processes are conspicuous with little biotic processes, despite conditions with sufficient bioavailable energy potentials and temperatures within the habitable range. However, there are still many uncertainties associated with the hypothesis presented here. It is not sufficient to clearly distinguish the geochemical processes in each of the spatio-temporally different stages of fluid-rock interactions beneath the SCS, such as metamorphism associated with subduction, fluid released from the plate boundary zone, extensive serpentinization at the wedge mantle, fluid maturation and cooling in the ascending pathway, episodic mud volcanism, and mass wasting of the SCS body. The behavior of sulfate in

subduction systems is a key factor for understanding the (bio) geochemical cycle at forearc geofluid systems. Constraint in keeping the co-existence of the (probably) slab-derived sulfate and abiotic  $\text{CH}_4$  in the SCS formation, unexpected due to the strong thermodynamic drive for their reaction, remains unidentified. Broadly speaking, abiotic organic synthesis associated with seafloor serpentinization has been considered to progress in many of the natural serpentinization-associated geofluid systems including the SCS, but has never been confirmed by multiple lines of solid evidences that serve to distinguish it from organic matter degradation and biological carbon fixation. Future studies of the SCS and other serpentinite mud volcanoes in the Mariana forearc are needed to refine conceptual models of reactions within these interesting features that link seafloor materials with the descending slab.

## Additional file

**Additional file 1: Table S1.** Results of chemical analyses of the CORK fluid (XLSX 49 kb)

## Abbreviations

CORK: Circulation Obviation Retrofit Kit; DPW: Deep porewater; IC: Ion chromatography; ICP-AES: Inductively coupled plasma atomic emission spectrometry; ICP-MS: Inductively coupled plasma mass spectrometry; ODP: Ocean Drilling Program; PVC: Polyvinyl chloride; ROV: Remotely operated vehicle; SCS: South Chamorro Seamount

## Acknowledgements

We thank the operation team of the ROV Hyper-Dolphin and the crews of R/V Natsushima for their skillful support during cruises NT09-1, NT09-7, NT12-04, and NT12-23. We also thank Dr. Uta Konno for gas and isotope analyses. Drs. Kentaro Nakamura, Takazo Shibuya, and Chong Chen are gratefully acknowledged for useful and fruitful discussions. SK thanks Prof. Gretchen Bernasconi-Green for providing space and opportunity to draft the manuscript as an academic visitor of ETH Zürich.

## Funding

This work was partly supported by JSPS KAKENHI Grant Number 25701004 (SK).

## Availability of data and materials

All analytical results of this study are included in the main text and tables.

## Authors' contributions

SK, JM, CGW, and KT proposed the topic, conceived, and designed the study. All authors joined cruises for sample collection. JM, YM, JSS, and CGW analyzed the samples and helped in their interpretation. JSS and CGW collaborated with the corresponding author (SK) in the construction of manuscript. All authors read and approved the final manuscript.

## Competing interests

The authors declare that they have no competing interest.

## Publisher's Note

Springer Nature remains neutral with regard to jurisdictional claims in published maps and institutional affiliations.

## Author details

<sup>1</sup>Department of Subsurface Geobiological Analysis and Research (D-SUGAR), Japan Agency for Marine-Earth Science and Technology (JAMSTEC), 2-15 Natsushima-cho, Yokosuka 237-0061, Japan. <sup>2</sup>Kochi Institute for Core Sample Research, Japan Agency for Marine-Earth Science and Technology (JAMSTEC), Nankoku, Kochi 783-8502, Japan. <sup>3</sup>Department Marine Chemistry and

Geochemistry (MC&G), Woods Hole Oceanographic Institution (WHOI), Woods Hole, MA 02543, USA. <sup>4</sup>Global Undersea Research Unit, University of Alaska Fairbanks, P. O. Box 475, Moss Landing, CA 95039, USA. <sup>5</sup>Institute of Geochemistry and Petrology, ETH Zürich, Zürich, Switzerland.

Received: 9 May 2018 Accepted: 19 October 2018

Published online: 14 November 2018

## References

- Alt JC, Shanks WC III (2006) Stable isotope compositions of serpentinite seamounts in the Mariana forearc: serpentinization processes, fluid sources and sulfur metasomatism. *Earth Planet Sci Lett* 242:272–285.
- Aoyama S, Nishizawa M, Miyazaki J, Shibuya T, Ueno Y, Takai K (2018) Recycled Archean sulfur in the mantle wedge of the Mariana Forearc and microbial sulfate reduction within an extremely alkaline serpentine seamount. *Earth Planet Sci Lett* 491:109–120.
- Barnes I, LaMarche J VC, Himmelberg G (1967) Geochemical evidence of present-day serpentinization. *Science* 156:830–832.
- Barnes I, O'neil JR, Trescases JJ (1978) Present day serpentinization in New Caledonia, Oman and Yugoslavia. *Geochim Cosmochim Acta* 42:144–145.
- Burruss RC, Laughrey CD (2010) Carbon and hydrogen isotopic reversals in deep basin gas: Evidence for limits to the stability of hydrocarbons. *Organic Geochemistry* 41:1285–1296. <https://doi.org/10.1016/j.orggeochem.2010.09.008>.
- Charlou JL, Donval JP, Fouquet Y, Jean-Baptiste P, Holm N (2002) Geochemistry of high H<sub>2</sub> and CH<sub>4</sub> vent fluids issuing from ultramafic rocks at the Rainbow hydrothermal field (36°14'N, MAR). *Chem Geol* 191:345–359.
- de Lange GJ, Cranston RE, Hydes DH, Boust D (1992) Extraction of pore water from marine sediments: a review of possible artifacts with pertinent examples from the North Atlantic. *Mar Geol* 109:53–76.
- Etiopie G, Sherwood Lollar B (2013) Abiotic methane on earth. *Rev Geophys* 51:1–24.
- France-Lanord C, Michard A, Karpoff AM (1992) Major element and Sr isotope composition of interstitial waters in sediments from leg 129: the role of diagenetic reactions. In: Larson RL, Lancelot Y et al (eds) *Proceedings of the Ocean Drilling Program Scientific Results*, vol 129, pp 267–281.
- Früh-Green GL, Kelley DS, Bernasconi SM, Karson JA, Ludwig KA, Butterfield DA, Boschi C, Proskurowski G (2003) 30,000 years of hydrothermal activity at the Lost City vent field. *Science* 301:495–498.
- Fryer P (2011) Serpentinite mud volcanism: observations, processes, and implications. *Annu Rev Mar Sci* 4:345–373.
- Fryer P, Mottl MJ (1997) "Shinkai 6500" investigations of a resurgent mud volcano on the Southeastern Mariana forearc. *JAMSTEC-R* 13:103–114.
- Fu Q, Sherwood Lollar B, Horita J, Lacrampe-Couloume G, Seyfried WE Jr (2007) Abiotic formation of hydrocarbons under hydrothermal conditions: constraints from chemical and isotope data. *Geochim Cosmochim Acta* 71:1982–1998.
- Gieskes J, Gamo T, Kastner M (1993) Major and minor element geochemistry of interstitial waters of site 808, Nankai trough: an overview. In: Hill IA, Taira A, Firth JV et al (eds) *Scientific results, Ocean Drilling Program, Leg 131. Ocean Drilling Program, College Station, Texas*, pp 387–396.
- Gieskes JM, Vrolijk P, Blank G (1990) Hydrogeochemistry of the Northern Barbados accretionary complex transect: Ocean Drilling Project Leg 110. *J Geophys Res* 95:8809–8818.
- Hensen C, Wallmann K (2005) Methane formation at Costa Rica continental margin - constraints for gas hydrate inventories and cross-décollement fluid flow. *Earth Planet Sci Lett* 236:41–60.
- Hirayama H, Fuse H, Abe M, Miyazaki M, Nakamura T, Nunoura T, Furushima Y, Yamamoto H, Takai K (2013) *Methylomarinum vadi* gen. nov. sp. Nov., a methanotroph isolated from two distinct marine environments. *Int J Syst Evol Microbiol* 63:1073–1082.
- Hirayama H, Sunamura M, Takai K, Nunoura T, Noguchi T, Oida H, Furushima Y, Yamamoto H, Oomori T, Horikoshi K (2007) Culture-dependent and -independent characterization of microbial communities associated with a shallow submarine hydrothermal system occurring within a coral reef off Taketomi Island, Japan. *Appl Environ Microbiol* 73:7642–7656.
- Homma A, Tsukahara H (2008) Chemical characteristics of hot spring water and geological environment in the northernmost area of the Itoigawa Shizuoka tectonic line. *Bull Earthw Res Inst Univ Tokyo* 83:217–225.
- Horibe Y, Craig H (1995) D/H fractionation in the system methane-hydrogen-water. *Geochim Cosmochim Acta* 59:5209–5217.
- Horita J (2001) Carbon isotope exchange in the system CO<sub>2</sub>-CH<sub>4</sub> at elevated temperatures. *Geochim Cosmochim Acta* 65:1907–1919.
- Hulme SM, Wheat CG, Fryer P, Mottl MJ (2010) Pore water chemistry of the Mariana serpentinite mud volcanoes: a window to the seismogenic zone. *Geochim Geophys Geosyst* 11:Q01X09. <https://doi.org/10.1029/2009GC002674>.
- Janecky DR, Seyfried WE Jr (1986) Hydrothermal serpentinization of peridotite within the oceanic crust: experimental investigations of mineralogy and major element chemistry. *Geochim Cosmochim Acta* 50:1357–1378.
- Kawagucci S, Miyazaki J, Noguchi T, Okamura K, Shibuya T, Watsuji T et al (2016) Fluid chemistry in the solitaire and dodo hydrothermal fields of the central Indian ridge. *Geofluids* 5:988–1005. <https://doi.org/10.1111/gfl.12201>.
- Kawagucci S, Toki T, Ishibashi J, Takai K, Ito M, Oomori T, Gamo T (2010) Isotopic variation of molecular hydrogen in 20°–375°C hydrothermal fluids as detected by a new analytical method. *J Geophys Res* 115:G03021–9. <https://doi.org/10.1029/2009JG001203>.
- Kawagucci S, Ueno Y, Takai K, Toki T, Ito M, Inoue K, Makabe A, Yoshida N, Muramatsu Y, Takahata N, Sano Y, Narita T, Teranishi G, Obata H, Nakagawa S, Nunoura T, Gamo T (2013) Geochemical origin of hydrothermal fluid methane in sediment-associated fields and its relevance to the geographical distribution of whole hydrothermal circulation. *Chem Geol* 339:213–225.
- Kelley DS, Karson JA, Blackman DK, Früh-Green GL, Butterfield DA et al (2001) An off-axis hydrothermal vent field near the Mid-Atlantic Ridge at 30°N. *Nature* 412:145–149.
- Kellmeyer J, Pockalny R, Adhikari RR, Smith DC, D'Hondt S (2012) Global distribution of microbial abundance and biomass in seafloor sediment. *PNAS* 109:16213–16216.
- Konn C, Charlou JL, Lohm NG, Mousis O (2015) The production of methane, hydrogen, and organic compound in ultramafic-hosted hydrothermal vents of the Mid-Atlantic Ridge. *Astrobiology* 15:381–399.
- Kumagai H, Nakamura N, Toki T, Morishita T, Okino K, Ishibashi J et al (2008) Geological background of the Kairei and Edmond hydrothermal fields along the Central Indian ridge: implications of their vent fluids' distinct chemistry. *Geofluids* 8:239–251.
- Mathrani IM, Boone DR, Mah RA, Fox GE, Lau PP (1988) *Methanohalophilus zhilinae* sp. Nov., an alkaliphilic, halophilic, methylotrophic methanogen. *Int J Syst Bacteriol* 38:139–142.
- McCollom TM (2008) Observational, experimental, and theoretical constraints on carbon cycling in Mid-Ocean Ridge hydrothermal systems. In: *Magma to microbe: modeling hydrothermal processes at ocean spreading centers geophysical monograph series*, vol 178, pp 193–213.
- McCollom TM (2013) Laboratory simulations of abiotic hydrocarbon formation in Earth's deep subsurface. *Rev Mineral Geochem* 75:467–494.
- McCollom TM, Bach W (2009) Thermodynamic constraints on hydrogen generation during serpentinization of ultramafic rocks. *Geochim Cosmochim Acta* 73:856–875.
- McCollom TM, Sherwood Lollar B, Lacrampe-Couloume G, Seewald JS (2010) The influence of carbon source on abiotic organic synthesis and carbon isotope fractionation under hydrothermal conditions. *Geochim Cosmochim Acta* 74:2717–2740.
- McDermott JM, Ono S, Tivey MK, Seewald JS, Shanks WC III, Solow AR (2015) Identification of sulfur sources and isotopic equilibria in submarine hot-springs using multiple sulfur isotopes. *Geochimica et Cosmochimica Acta* 160:169–187. <https://doi.org/10.1016/j.gca.2015.02.016>.
- Miyazaki J, Makabe A, Matsui Y, Ebina N, Tsutsumi S, Ishibashi J, Chen C, Kaneko S, Takai K, Kawagucci S (2017) WHATS-3: an improved flow-through multi-bottle fluid sampler for Deep-Sea Geofluid research. *Front Earth Sci* 5:45. <https://doi.org/10.3389/feart.2017.00045>.
- Morono Y, Inagaki F (2010) Automatic Slide-Loader Fluorescence Microscope for Discriminative Enumeration of Subseafloor Life. *Scientific Drilling* 9:32–36. <https://doi.org/10.5194/sd-9-32-2010>.
- Morono Y, Terada T, Kallmeyer J, Inagaki F (2013) An improved cell separation technique for marine subsurface sediments: applications for high-throughput analysis using flow cytometry and cell sorting. *Environ Microbiol* 2:2841–2849. <https://doi.org/10.1111/1462-2920.12153>.
- Morono Y, Terada T, Masui N, Inagaki F (2009) Discriminative detection and enumeration of microbial life in marine subsurface sediments. *The ISME Journal* 3:503–511. <https://doi.org/10.1038/ismej.2009.1>.

- Mottl MJ, Komor SC, Fryer P, Moyer CL (2003) Deep-slab fluids fuel extremophilic archaea on a Mariana forearc serpentinite mud volcano: Ocean Drilling Program Leg 195. *Geochem Geophys Geosyst* 4:9009.
- Mottl MJ, Wheat CG, Fryer P, Gharib J, Martin J (2004) Chemistry of springs across the Mariana forearc shows progressive devolatilization of the subduction plate. *Geochim Cosmochim Acta* 68:4915–4933.
- Nakagawa S et al (2006) Microbial community in black rust exposed to hot ridge flank crustal fluids. *Appl Environ Microbiol* 72:6789–6799.
- Nakamura K, Takai K (2014) Theoretical constraints of physical and chemical properties of hydrothermal fluids on variations in chemolithotrophic microbial communities in seafloor hydrothermal systems. *Prog Earth Planet Sci* 1:5.
- Nigro LM, Harris K, Orcutt BN, Hyde A, Clayton-Luce S, Becker K, Teske A (2012) Microbial communities at the borehole observatory on the Costa Rica Rift flank (Ocean Drilling Program Hole 896A). *Front Microbiol* 3:232. <https://doi.org/10.3389/fmicb.2012.00232>.
- Nunoura T, Takaki Y, Kazama H, Hirai M, Ashi J, Imachi H, Takai K (2012) Microbial diversity in deep-sea methane seep sediments presented by SSU rRNA gene tag sequencing. *Microbes Environ* 27:382–390. <https://doi.org/10.1264/jsm.2012.0232>.
- Ohara Y et al (2012) A serpentinite-hosted ecosystem in the southern Mariana Forearc. *Proc Natl Acad Sci U S A* 109:2831–2835. <https://doi.org/10.1073/pnas.1112005109>.
- Okumura T, Kawagucci S, Saito Y, Matsui Y, Takai K, Imachi H (2016b) Hydrogen and carbon isotope systematics in hydrogenotrophic methanogenesis under H<sub>2</sub>-limited and H<sub>2</sub>-enriched conditions: implications for the origin of methane and its isotopic diagnosis. *Prog Earth Planet Sci* 3:14.
- Okumura T et al (2016a) Brucite chimney formation and carbonate alteration at the Shinkai seep field, a serpentinite-hosted vent system in the southern Mariana forearc. *Geochem Geophys Geosyst* 17. <https://doi.org/10.1002/2016GC006449>.
- Onishi Y, Yamanaka T, Okumura T, Kawagucci S, Watanabe HK, Ohara Y (2018) Evaluation of nutrient and energy sources of the deepest known serpentinite-hosted ecosystem using stable carbon, nitrogen, and sulfur isotopes. *PLoS One* 13(6):e0199000.
- Orphan VJ, House CH, Hinrichs K-U, McKeegan KD, DeLong EF (2001) Methane-consuming archaea revealed by directly coupled isotopic and phylogenetic analysis. *Science* 293:484–487.
- Penning H, Plugge CM, Galand PE, Conrad R (2005) Variation of carbon isotope fractionation in hydrogenotrophic methanogenic microbial cultures and environmental samples at different energy status. *Glob Chang Biol* 11:2103–2113.
- Pester NJ, Conrad ME, Knauss KG, DePaolo DJ (2018) Kinetics of D/H isotope fractionation between molecular hydrogen and water. *Geochim Cosmochim Acta* 242:191–212.
- Proskurowski G, Lilley MD, Seewald JS, Fru h-Green GL, Olson EJ, Lupton JE, Sylva SP, Kelley DS (2008) Abiogenic Hydrocarbon Production at Lost City Hydrothermal Field. *Science* 319:604–607. <https://doi.org/10.1126/science.1151194>.
- Redfield AC (1958) The biological control of chemical factors in the environment. *Am Sci* 46:205–221.
- Reeves E, Seewald JS, Sylva SP (2012) Hydrogen isotope exchange between n- alkanes and water under hydrothermal conditions. *Geochim Cosmochim Acta* 77:582–599.
- Russell MJ et al (2014) The drive to life on wet and icy worlds. *Astrobiology* 14: 308–343.
- Saegusa S, Tsunogai U, Nakagawa F, Kaneko S (2006) Development of a multibottle gas-tight fluid sampler WHATS II for Japanese submersibles/ROVs. *Geofluids* 6:234–240.
- Sano Y, Marty B (1995) Origin of carbon in fumarolic gas from island arcs. *Chem Geol* 119:265–274.
- Schrenk MO, Brazelton WJ, Lang SQ (2013) Serpentinization, carbon, and deep life. *Rev Mineral Geochem* 75:575–606.
- Seewald JS, Doherty KW, Hammar TR, Liberatore SP (2001) A new gas-tight isobaric sampler for hydrothermal fluids. *Deep Sea Res* 49:189–196. [https://doi.org/10.1016/S0967-0637\(01\)00046-2](https://doi.org/10.1016/S0967-0637(01)00046-2).
- Seewald JS, Seyfried WE Jr, Shanks WC III (1994) Variations in the chemical and stable isotope composition of carbon and sulfur species during organic-rich sediment alteration: an experimental and theoretical study of hydrothermal activity at Guaymas Basin, Gulf of California. *Geochim Cosmochim Acta* 58: 5065–5082.
- Sessions AL, Sylva SP, Summons RE, Hayes JM (2004) Isotopic exchange of carbon-bound hydrogen over geological timescales. *Geochim Cosmochim Acta* 68:1545–1559.
- Seyfried WE Jr, Foustoukos DI, Fu Q (2007) Redox evolution and mass transfer during serpentinization: an experimental and theoretical study at 200 °C, 500 bar with implications for ultramafic-hosted hydrothermal systems at Mid-Ocean Ridge. *Geochim Cosmochim Acta* 71:3872–3886.
- Seyfried WE Jr., Pester NJ, Ding K, Rough M (2011) Vent fluid chemistry of the Rainbow hydrothermal system (36°N, MAR): Phase equilibria and in situ pH controls on subseafloor alteration processes. *Geochimica et Cosmochimica Acta* 75:1574–1593. <https://doi.org/10.1016/j.gca.2011.01.001>.
- Shibuya T, Komiya T, Takai K, Maruyama S, Russell MJ (2017) Weak hydrothermal carbonation of the Ongeluk volcanics: evidence for low CO<sub>2</sub> concentrations in seawater and atmosphere during the Paleoproterozoic global glaciation. *Prog Earth Planet Sci* 4:31. <https://doi.org/10.1186/s40645-017-0145-6>.
- Sherwood Lollar B, Westgate TD, Ward JA, Slater GF, Lacrampe-Couloume G (2002) Abiogenic formation of alkanes in the Earth's crust as a minor source for global hydrocarbon reservoirs. *Nature* 416:522–524. <https://doi.org/10.1038/416522a>.
- Shipboard Sci. Party (2002) In: Peters LL (ed) Site 1200. *Proc. Ocean Drill. Prog. Initial Rep., Vol. 195. Ocean Drill. Prog./Texas A&M Univ, College Station.* <https://doi.org/10.2973/odp.proc.ir.195.103.2002>.
- Stern RJ, Ren M, Kelley KA, Ohara Y, Martinez F, Bloomer SH (2014) Basaltic volcanoclastics from the Challenger Deep forearc segment, Mariana convergent margin: Implications for tectonics and magmatism of the southernmost Izu-Bonin-Mariana arc. *Island Arc* 23:368–382. <https://doi.org/10.1111/iar.12088>.
- Stolper DA, Lawson M, Davis CL, Ferreira AA, Santos Neto EV, Ellis GS, Lewan MD, Martini AM, Tang Y, Schoell M, Sessions AL, Eiler JM (2014) Formation temperatures of thermogenic and biogenic methane. *Science* 344:1500–1503.
- Suda K, Ueno Y, Yoshizaki M, Nakamura H, Kurokawa K, Nishiyama E, Yoshino K, Hongoh Y, Kawachi K, Omori S, Yamada K, Yoshida N, Maruyama S (2014) Origin of methane in serpentinite-hosted hydrothermal systems: The CH<sub>4</sub>–H<sub>2</sub>–H<sub>2</sub>O hydrogen isotope systematics of the Hakuba Happo hot spring. *Earth and Planetary Science Letters* 386:112–125. <https://doi.org/10.1016/j.epsl.2013.11.001>
- Takai K, Gamo T, Tsunogai U, Nakayama N, Hirayama H, Nealson KH, Horikoshi K (2004) Geochemical and microbiological evidence for a hydrogen-based, hyperthermophilic subsurface lithoautotrophic microbial ecosystem (HyperSLiME) beneath an active deep-sea hydrothermal field. *Extremophiles* 8:269–282.
- Takai K, Moser DP, Onstott TC, Spoelstra N, Pfiffner SM, Dohnalkova A, Fredrickson JK (2001) *Alkaliphilus transvaalensis* gen. nov., sp. Nov., an extremely alkaliphilic bacterium isolated from a deep South African gold mine. *Int J Syst Evol Microbiol* 51:1245–1256.
- Takai K, Moyer CL, Miyazaki M, Nogi Y, Hirayama H, Nealson KN, Horikoshi K (2005) *Marinobacter alkaliphilus* sp. Nov., a novel alkaliphilic bacterium isolated from subseafloor alkaline serpentine mud from Ocean Drilling Program Site 1200 at South Chamorro Seamount, Mariana Forearc. *Extremophiles* 9:17–27.
- Takai K, Nakamura K, Suzuki K, Inagaki F, Nealson KH, Kumagai H (2006) Ultramafic-Hydrothermalism-Hydrogenesis-HyperSLiME (UltraH3) linkage: a key insight into early microbial ecosystem in the Archean deep-sea hydrothermal systems. *Paleontological Res* 10:269–282.
- Takai K, Nakamura K, Toki T, Tsunogai U, Miyazaki M, Miyazaki J, Hirayama H, Nakagawa S, Nunoura T, Horikoshi K (2008) Cell proliferation at 122 °C and isotopically heavy CH<sub>4</sub> production by a hyperthermophilic methanogen under high-pressure cultivation. *Proc Natl Acad Sci U S A* 105:10949–10954.
- Tishchenko P, Hensen C, Wallmann K, Wong CS (2005) Calculation of the stability and solubility of methane hydrate in seawater. *Chem Geol* 219:37–52.
- Ueda H, Shibuya T, Sawaki Y, Saitoh M, Takai K, Maruyama S (2016) Reactions between komatiite and CO<sub>2</sub>-rich seawater at 250 and 350 °C, 500 bars: implications for hydrogen generation in the Hadean seafloor hydrothermal system. *Progress in Earth and Planet Sci* 3:35. <https://doi.org/10.1186/s40645-016-0111-8>.
- Valentine DL, Chidthaisong A, Rice A, Reeburgh WS, Tyler SC (2004) Carbon and hydrogen isotope fractionation by moderately thermophilic methanogens. *Geochim Cosmochim Acta* 68:1571–1590.
- Wang DT, Gruen DS, Lollar BS, Hinrichs KU, Stewart LC, Holden JF, Hristov AN, Pohlman JW, Morrill PL, Konneke M, Delwiche KB, Reeves EP, Sutcliffe CN, Ritter DJ, Seewald JS, McIntosh JC, Hemond HF, Kubo MD, Cardace D,

- Hoehler TM, Ono S (2015) Nonequilibrium clumped isotope signals in microbial methane. *Science* 348:428–431. <https://doi.org/10.1126/science.aaa4326>.
- Wheat CG, Fryer P, Fisher AT, Hulme S, Jannasch H, Mottl MJ, Becker K (2008) Borehole observations of fluid flow from South Chamorro Seamount, an active serpentinite mud volcano in the Mariana forearc. *Earth Planet Sci Lett* 267:401–409.
- Wiesenburg DA, Guinasso NL Jr (1979) Equilibrium solubilities of methane, carbon monoxide, and hydrogen in water and sea water. *J Chem Eng Data* 24:356–560.

**Submit your manuscript to a SpringerOpen<sup>®</sup> journal and benefit from:**

- ▶ Convenient online submission
- ▶ Rigorous peer review
- ▶ Open access: articles freely available online
- ▶ High visibility within the field
- ▶ Retaining the copyright to your article

---

Submit your next manuscript at ▶ [springeropen.com](https://www.springeropen.com)

---